THE APICAL MEMBRANE PROTEIN PODOCALYXIN ACTS AS AN ANTI-ADHESIN IN EPITHELIAL OVARIAN CARCINOMA

by

JANE ALEXANDRA CIPOLLONE

B.Sc., The University of British Columbia, 2003

A THESIS SUBMITTED IN PARTIAL FULFILLMENT
OF THE REQUIREMENTS FOR THE DEGREEOF
MASTER OF SCIENCE

in

THE FACULTY OF GRADUATE STUDIES

(Anatomy)

THE UNIVERSITY OF BRITISH COLUMBIA

December 2006

© Jane Alexandra Cipollone, 2006

ABSTRACT

Podocalyxin is a heavily sialylated and sulfated integral membrane protein with anti-adhesive properties that contributes to apical domain formation in normal, polarized epithelial cells. Immunohistochemical analysis of an outcome-linked ovarian tumour microarray (TMA) revealed that podocalyxin was expressed in the majority of lesions but showed no significant correlation with poor outcome. Podocalyxin expression was most prevalent in serous tumours where it was often apically localized in low-grade well-differentiated tumours. In the normal ovary, podocalyxin expression was moderate and localized to the free peritoneal surface of normal ovarian surface epithelia (OSE), serving to distinguish the OSE from its underlying stroma. Interestingly, podocalyxin was apically localized in dysplastic, columnar OSE suggesting that it may serve as a marker of polarity early in the carcinogenic process.

After characterizing podocalyxin expression in a variety of ovarian carcinoma cell lines, OVCAR-3, a low podocalyxin expressing cell line, was forced to overexpress the mouse podocalyxin cDNA. Forced overexpression of podocalyxin did not disrupt cell-cell junctions in polarized monolayers. However, it did disrupt cohesive cell-cell aggregation in suspension. In addition, podocalyxin overexpression in depolarized monolayers disrupted cell:subtratum adhesion. Podocalyxin overexpression caused a marked decrease in cell adhesion to fibronectin, mesothelial cells and to anti-$\beta 1$ integrin antibody-coated wells, suggesting that high levels of podocalyxin may interfere with integrin engagement.

To investigate the consequences of podocalyxin overexpression on β1 integrin localization in polarized monolayers and 3D cell clusters, dual immunofluorescence staining was performed for podocalyxin/β1 integrin. Podocalxyin overexpressing monolayers targetted podocalyxin to the apical membrane, resulting in a subtle depletion of β1 integrin from this site. In non-polar 3D cultures, podocalyxin overexpressing cell clusters mislocalized podocalxyin to the cell-matrix interface causing β1 integrin depletion from this membrane domain. Therefore, as a cell-ECM disrupting anti-adhesin, mislocalized podocalyxin may promote the dissemination of primary tumour nodules into the peritoneal cavity by interfering with integrin engagement at the tumour:ECM interface.

TABLE OF CONTENTS

LIST OF FIGURES

LIST OF ABBREVIATIONS

APC   allophycocyanin
aPKC   atypical protein kinase C
BSA   bovine serum albumin
CA125   cancer antigen 125
CHO   chinese hamster ovary
CMFDA   5-chloromethylfluorescein diacetate
CRB   crumbs
DABCO   1,4-diazabicyclo[2.2.2]octane
DAPI   4'6-Diamidino-2-phenylindole
DMEM   Dulbecco's modified Eagle's media
DTHL   Asp-Thr-His-Leu
ECL   enhanced chemiluminescence
ECM   extracellular matrix
EHS   Engelbreth-Holm-Swarm
EMT   epithelial-mesenchymal transition
ERK   extracellular regulated kinase
ERM   ezrin-radixin-moesin
FACs   fluorescence automated cell sorting
FBS   fetal bovine serum
gp135   glycoprotein 135
HCM   high calcium media
HRP   horseradish perodixase
IgG   Immunoglobulin G
IL-3   interleukin-3
IL-6   interleukin-6
IL-8   interleukin-8
JAM   junctional adhesion molecule
LCM   low calcium media
LGL   lethal giant larva
MDCK   Madin-Darby canine kidney
Ms   mouse
MUC1   mucin-1
NHERF   sodium-proton exchange regulatory factor
NaAzide   sodium azide
NGS   normal goat serum
OSE   ovarian surface epithelium
PAR   partitioning defective
PDZ   PSD-95/Disc-large/ZO-1
Rb   rabbit
Rho   ras-homology
SAGE   serial analysis of gene expression
SAv-APC   streptavidin-allophycocyanin
SD   standard deviation
SMP   skim milk powder

| TGF-β | transforming growth factor beta |
| ZO-1 | zonula occludens-1 |

ACKNOWLEDGEMENTS

1. INTRODUCTION

Polarity in Ovarian Carcinoma Progression

Although the loss of epithelial differentiation and apical-basal polarity are hallmarks

of early stage carcinogenesis in most epithelially-derived tumours, early stage epithelial

ovarian carcinoma provides a notable exception to this general rule. Rather than being

characterised by a loss of polarity, putative pre-malignant ovarian epithelial lesions undergo

an increase in differentiative polarity relative to their proposed precursor cells. Substantial

evidence supports the notion that epithelial ovarian carcinomas arise from the ovarian surface

epithelium (OSE), a simple, modified mesothelium that covers the surface of the ovary

(Feeley and Wells, 2001; Orsulic et al., 2002; Scully, 1995). The OSE is poorly differentiated

and characterized by an absence of E-cadherin expression, thus serving as a unique example

of an epithelium that does not maintain E-cadherin-mediated cell-cell adhesions (Maines-

Bandiera and Auersperg, 1997; Sundfeldt et al., 1997). The OSE also exhibits both epithelial

and mesenchymal characteristics, which likely reflects its primitive differentiation state. For

example, the OSE expresses the epithelial intermediate filament keratin, yet also produces

the mesenchymal intermediate filament vimentin, stromal collagen and matrix

metalloproteases (Auersperg et al., 2001). Importantly, the primitive differentiation state of

the OSE contributes to its phenotypic plasticity, permitting the resting OSE, which is

normally stationary and epithelial, to adopt mesenchymal properties during post-ovulatory

wound repair and rapidly migrate to repair defects in the surface of the ovary. It is

hypothesized that repeated rupture and repair during ovulation increases the propensity of the

OSE to undergo malignant transformation (Tortolero-Luna and Mitchell, 1995). Analysis of

1

contralateral ovaries in patients with unilateral ovarian cancer has revealed that potentially pre-malignant surface clefts and inclusion cysts are more prevalent (Mittal et al., 1993). Interestingly, OSE-derived cells lining the latter structures are ten times more likely to undergo differentiative tubal metaplasia than the normal OSE (Mittal et al., 1993; Tresserra et al., 1998). As a result, potenitally pre-malignant OSE-derived cells that become trapped within inclusion cysts or surface clefts often exhibit a phenotypically restricted, differentiated, columnar morphology with evident apical-basal polarity (Feeley and Wells, 2001)

The OSE arises from the coelomic epithelium, adjacent to the epithelium that gives rise to the Mullerian ducts. The Mullerian duct-derived epithelium develops into the epithelial lining of the fallopian tubes, uterus and endocervix and epithelial ovarian carcinomas are classified into histological subtypes based on their phenotypic resemblance to these tissues. For example, serous carcinomas resemble the epithelia of the fallopian tube, while endometriod carcinomas resemble the epithelia of the endometrium and mucinous carcinomas resemble the epithelia of the endocervix (Barber, 1993). Thus, the pre-neoplastic metaplastic changes associated with ovarian carcinogenesis involve an acquisition of the polarized, differentiated phenotype of developmentally-related Mullerian duct-derived epithelia. Along with a columnar morphology, this phenotype is characterized by the induction of E-cadherin expression and expression of CA125, a normal differentiation marker of Mullerian duct-derived epithelia absent in the normal OSE (Salazar et al., 1996).

In addition to metaplastic inclusion cysts and surface clefts, E-cadherin expression is a characteristic of tumours of low malignant potential and true ovarian carcinoma (Darai et al., 1997; Davidson et al., 2000; Davies et al., 1998; Hough et al., 2000; Inoue et al., 1992; Maines-Bandiera and Auersperg, 1997; Sundfeldt et al., 2001; Sundfeldt et al., 1997). E-cadherin expression is thought to play an inductive role in the acquistion of a differentiated epithelial phenotype that is associated with metaplasia (Auersperg et al. 1999). When immortalized OSE cells were forced to express E-cadherin they assembled functional adherens junctions and acquired the characteristics of of pre-neoplastic, metaplastic OSE and primary carcinomas in that they adopted a stationary, epithelial morphology and expressed CA125. Along with displaying the characteristics of Mullerian-duct derived epithelia, force expression of E-cadherin caused the OSE-derived cells to express the tight junction protein occludin (Auersperg et al., 1999). Another report using serial analysis of gene expression (SAGE) revealed that expression of tight junction proteins claudin-3 and claudin-4 was upregulated in primary ovarian carcinoma relative to non-transformed ovarian epithelia (Hough et al., 2000). Taken together, this suggests that along with the acquisition of Mullerian duct-derived epithelial characteristics induced by E-cadherin expression, increased tight junction protein expression may contribute to the differentiative polarization of metaplastic OSE and borderline tumours. This is consistent with E-cadherin's central role as a component of adherens junctions, which are thought to serve as primary landmarks during cell polarization, and are prerequisite for the assembly of tight junctions (Gumbiner, 1988). Thus, the differentiation and polarization exhibited early in ovarian carcinogenesis provides a notable exception to the dogma that carcinoma progression involves an early loss of polarity and a progressive loss of differentiaton.

Given the hallmarks of carcinoma progression in other tissues, the increase in differentiation and polarization in epithelial ovarian carcinoma seems paradoxical. However, given the unusual route of metastatic dissemination of ovarian carcinoma, E-cadherin-mediated adhesion may confer a selective advantage to these cells. Rather than relying primarily on entry into the vasculature for dissemination from primary sites, primary ovarian carcinoma nodules are often shed from the surface of the ovary into the peritoneal cavity. The mechanism responsible for this shedding is, as yet, unknown. However, once free in the peritoneal cavity, these cells exist as anchorage-independent, suspended effusions. The maintenance of E-cadherin-mediated cell-cell contacts by suspended ovarian carcinoma cells may enable them to evade apoptotic anoikis since E-cadherin mediated adhesion induces downstream survival and proliferation signals in ovarian cancer cells (Reddy et al., 2005) . In later stages of ovarian carcinoma progression, suspended effusions may attach and invade into the peritoneum, at which point dissolution of cell-cell adhesion may facilitate invasion. Therefore, like carcinoma progression in other tissues where E-cadherin acts as a tumour suppressor (Birchmeier and Behrens, 1994), the late metastatic stages of ovarian carcinoma may also be characterized by a loss of E-cadherin expression or function (Naora and Montell, 2005).

As mentioned above, the exact molecular mechanisms underlying the early stages of ovarian carcinogenesis are poorly understood. This is largely due to the lack of a definitive experimental model that recapitulates the early events of the disease. In addition, early detection and reliable screening methods for the disease are problematic. Therefore ovarian cancer is usually detected when it has spread beyond the ovaries and prognosis is poor. As

such, a better understanding of the precise molecular events that enable tumour formation and its dissemination beyond the ovary are warranted. Given that the early stages of ovarian carcinogenesis are characterised by an induction of E-cadherin-mediated differentiation, factors that promote the evolution of ovarian carcinoma may not necessarily function in conventional pathways towards metastasis. A possible example of such tumour-promoting factors could be a cell polarity determinant. For example, high levels of expression of a PAR polarity complex component in ovarian carcinoma correlate with loss of apical-basal polarity and decreased disease-specific survival (Eder et al., 2005). Therefore, factors that influence polarity may exhibit dual roles whereby they promote the early induction of polarity in ovarian carcinoma as well as potentially contribute to loss of polarity if misregulated.

Epithelial Cell Polarity

Extracellular adhesive interactions mediate the organization of single cells into the specialized architecture characteristic of each tissue. Epithelial tissues are composed of closely arranged cells that occur in one or more layers and cover the surface of the body or line internal cavities or tubes. Functionally, epithelial sheets delineate internal compartments and maintain their distinct composition by acting as a selective barrier to the exchange of molecules and ions between them. Structurally, epithelial sheets rely on elaborate cell junctions to allow the close apposition of cells and to provide mechanical links to maintain the structural integrity of the tissue and control the movement of solutes across the tissue (Yeaman et al., 1999). The establishment of apical-basal polarity is critical for generating positional assymetry across these epithelia. Polarized epithelial cells maintain distinct plasma membrane domains with their free, apical surface facing the external

environment or lumen, while the bounded, basolateral membrane domain contacts neighbouring cells and the extracellular matrix (ECM) substratum (Yeaman et al., 1999). Cell polarization involves two important stages. First, the cell must establish its axis, next the cell must generate and then maintain molecular asymmetry along this axis. This process depends on and is regulated by spatial cues from initial cell-cell and cell-ECM adhesions to direct the assembly of junctional complexes. Junctional complexes that are of critical importance for apical-basal polarity include adherens junctions and tight junctions (Nelson, 2003).

Cell-cell and cell-ECM junctions have the same basic framework and share similar general components. Integral membrane proteins mediate extracellular binding and interact with cytosolic binding partners. These associated cytosolic proteins act as scaffolds to provide a structural bridge to link extracellular binding to the cytoskeleton. In addition, cytosolic proteins associated with junctional complexes can function as adaptors by virtue of their multiple protein-protein interaction domains which enable the formation of multivalent protein complexes and offer potential sites for interlinking different junctional complexes. Scaffolding proteins have the potential to enhance the cellular response by initiating the formation of complexes to recruit and localize signaling networks or transcriptional regulators to junctional complexes to elicit appropriate changes in cell behaviour (Nelson, 2003). In addition, scaffolding proteins may bind to the actin cytoskeleton, the dynamics of which are regulated by the Rho family of small GTPases, which includes Rho, Rac1 and Cdc42. The recruitment of regulatory proteins to junctional complexes controls the activation state of Rho GTPases, and thus their ability to direct actin dynamics, which is critical for

cytoskeletal rearrangements that stabilize junctional complexes in time and space (Fukata and Kaibuchi, 2001).

Determinants of apical-basal polarity: cell-cell junctions

Appropriately localized cell-cell junctions are a prerequisite for epithelial cell polarization. During polarization, the cell adopts an asymmetric shape with unevenly distributed organelles and cytoskeletal networks. Tight junctions are adhesion complexes that encircle the apical aspect of the lateral membrane. They function as a paracellular diffusion barrier to regulate permeability of the epithelial sheet. In addition, they act as an intramembrane diffusion barrier to segregate the composition of the apical and basolateral membrane domains. Full polarization requires the assembly of tight junctions to demarcate the apical and basolateral membrane and this depends on the assembly of adherens junctions as well as cell-substratum interactions (Wang et al., 1990).

Calcium-dependent homophilic interactions between neighbouring cells are mediated by E-cadherin, the transmembrane component of adherens junctions, which direct co-ordinated cell-cell adhesion at the lateral membrane. The sequential binding of catenins to E-cadherin's cytosolic tail creates a bridge between extracellular adhesion and intracellular adaptor proteins and the cytoskeleton to yield a mature adherens junction consisting of continuous belt junctions around the apex of the cell (Adams et al., 1998; Yonemura et al., 1995). Assembly of cell junctional complexes is triggered by initial contacts mediated by E-cadherin and nectins at the surface of neighbouring cells resulting in the assembly of a primordial junction. Components of adherens junctions (catenins and afadin/AF-6) and tight

junctions (JAM, occludin, claudin, ZO-1) are recruited to this primordial junction. During adherens junction assembly, E-cadherin and nectin mediated contacts act as a cell surface landmark, generating molecular cues to trigger other networks that are required for cellular asymmetry such as recruitment of polarity complexes (Izumi et al., 1998) and assembly of tight junctions (Gumbiner, 1988). In this way, adherens junctions are thought to serve at the top of the epithelial polarization hierarchy, since the assembly of other complexes required for polarization relies on prior adherens junction assembly (Nelson, 2003). Importantly, adherens junction assembly stimulates local activation of Cdc42 and Rac1, which promotes the functionality of the "PAR polarity complex" apical to adherens junctions, that ultimately regulates cell junction localization. (Knust and Bossinger, 2002).

Regulators of junction localization: polarity complexes

Evidence from genetic screens in *Drosophila* and *C. elegans* has identifed classes of proteins in the apical junctional complex that regulate the establishment and maintenance of epithelial cell polarity. Experiments with mammalian epithelial cells have confirmed these classes of polarity complexes are evolutionarily conserved. The PAR polarity complex consists of Par3/Par6/aPKC. Functionality of the PAR complex at adherens junctions is promoted by active Cdc42, which binds to Par6 leading to activation of aPKC ((Joberty et al., 2000). Assembly of active PAR complexes apical to adherens junctions is important for assembling tight junctions and establishing and maintaining cell polarity (Joberty et al., 2000; Lin et al., 2000; Suzuki et al., 2001). The finding that JAMs, a component of tight junctions, could recruit the aPKC/Par-3/Par-6 complex to sites of cell-cell contact has led to the development of a model that partly outlines how initial cell-cell contacts results in tight

junction assembly, and ultimately apical-basal polarization. Following homotypic E-cadherin and nectin interactions on the surface of adjacent cells, a primordial junction that contains both adherens junction and tight junction components is assembled. The cytoplasmic domains of nectin and E-cadherin associate indirectly: adaptor protein AF-6 binds β-catenin at adherens junctions and binds to afadin, which binds to the C-terminus of nectin (Yokoyama et al., 2001). During adherens junction and tight junction assembly in vertebrate MDCK cells, E-cadherin, α-catenin, β-catenin and ZO-1 have been shown to localize to these primordial junctions (Ando-Akatsuka et al., 1999). During adherens junction assembly, JAM-1 is recruited apical to E-cadherin adhesion sites to sites of nectin adhesion. JAM-1 and nectin interact indirectly through their respective cytoplasmic tail binding proteins ZO-1 and AF-6 (Fukuhara et al., 2002). JAMs are thought to be the first transmembrane tight junction component recruited, shortly thereafter to be followed by claudins and occludin (Ebnet et al., 2004). Along with JAM recruitment, the aPKC/Par-3/Par-6 complex is recruited to primordial junctions (Ebnet et al., 2001). Adhesion mediated activation of Cdc42 promotes stability of adherens junctions as well activation of aPKC complexed to Par-3/Par-6. Although the molecular mechanisms underlying this process are poorly understood, these steps lead to maturation of the junctional complex and formation of distinct adherens junction and tight junction complexes (Matter and Balda, 2003).

Initiator of polarity: ECM/integrins

Sheets of interconnected epithelial cells are attached to a specialized extracellular matrix, the basement membrane, which provides a scaffold for the organization of cells into tissues. Integrins constitute a large family of transmembrane cell surface receptors that bind

and mediate adhesion to extracellular matrix components. Integrins are heterodimers composed of an alpha and beta subunit, which are transmembrane proteins with a single membrane-spanning domain. Following integrin engagement by ECM, a submembrane plaque consisting of adaptor proteins is assembled and stabilized through linkage to the actin cytoskeleton. This generates spatial cues that are translated into the establishment of an early axis of polarity (Ojakian and Schwimmer, 1994). Using MDCK cells, changes in the axis of polarity were manipulated by changing the orientation of the ECM relative to different membrane domains (Schwimmer and Ojakian, 1995). This confirmed that cell-ECM adhesion, mediated by integrins, provides a spatial cue for the establishment of the axis of polarity in polarized epithelial cells.

Experiments employing a dominant-negative Rac1 construct in developing MDCK cysts embedded in collagen gel have revealed a central role for this small GTPase in epithelial polarization (O'Brien et al., 2001). These experiments revealed that Rac1 is required for proper orientation of the apical pole by promoting a pathway that leads to laminin assembly at the basal surface (O'Brien et al., 2001). Subsequent work with MDCK cysts showed β1 integrin interaction with collagen I initiates a signalling pathway that leads to the activation of Rac1 and subsequent laminin organization into a basement membrane network. Properly assembled laminin provides a spatial cue that orients the axis of polarity such that it is coordinated with surrounding tissue architecture. Assembled laminin is proposed to induce a signalling pathway involving an integrin receptor for laminin that may stimulate Cdc42 activity at cell-ECM adhesion sites. Cdc42 may subsequently act as an intermediate to influence the Par3/Par6/aPKC complex to translate cues specifying the axis

of polarity into the establishment of membrane asymmetry (Zegers et al., 2003). Although it has been well established that ECM/integrins are responsible for relaying external cues that establish the axis of polarity, precisely how signaling pathways initiated at the cell-ECM boundary are able to execute polarization of the cell is not clear. The contribution of integrins in generating polarity cannot be separated from other interactions that occur simultaneously like contact between neighbouring cells. How adherens junctions and integrins are co-ordinated in generating polarity is not known. Whether integrin-mediated adhesion and adherens junctions reciprocate in signaling polarity or have a hierarchical relationship is also poorly understood (Weaver et al., 1997).

Modulators of polarity

Contrary to most models which place adherens junctions at the top of an epithelial polarization hierarchy, recent evidence suggests that certain polarity determinants may be capable of executing epithelial polarization in single cells. LKB1 is a serine/threonine kinase that is essential for the establishment of cell polarity in *C.elegans* and *Drosophila* (Martin and St Johnston, 2003; Watts et al., 2000) and it is a tumour suppressor that is mutated in the germline of Peutz-Jeghers cancer syndrome patients (Hemminki et al., 1998; Jenne et al., 1998). It is thought that a loss of LKB1 disrupts cell polarity thereby leading to cell transformation (Baas et al., 2004). In contrast, activation of LKB1 in single, attached cells executes polarization as characterized by remodelling of the actin cytoskeleton into an apical brush border and the redistribution of tight junction associated ZO-1 and adherens junction associated p120 to surround an actin cap. Additionally, these single, attached cells are able to sort and segregate their apical and basolateral membrane domains. Proposed candidate

effectors for LKB1 are Rho family GTPases which are likely to mediate actin cytoskeletal rearrangements necessary for actin cap/microvilli formation and could also potentially regulate the PAR complex. With LKB1-induced microvilli formation in these single cells there is potential for recruitment and retention of apical proteins to this cell surface landmark. One microvillus component which could retain apical surface proteins is the actin-binding protein ezrin (Baas et al., 2004; Berryman et al., 1993). Recently, podocalyxin, an apical membrane protein, was shown to localize to a pre-apical membrane domain in single, attached cells, supporting this model where membrane assymmetry may occur in the absence of cell-cell contacts (Meder et al., 2005). The formation of a basal attachment site is proposed to lead to the assembly of an apical counterpart consisting of a scaffold formed by apical membrane proteins such as podocalyxin. Interestingly, podocalyxin has also been demonstrated to participate in the formation of microvilli and to interact with ezrin (Nielsen et al., 2005), two events proposed to promote polarization downstream of LKB1 (Baas et al., 2004). Therefore, LKB1 and podocalyxin are examples of putative polarity modulating proteins that function independently of conventional epithelial polarization pathways initiated by adherens junctions. We found that podocalyxin is overexpressed in a subset of metastatic breast tumours (Somasiri et al., 2004) and I have found that it is highly expressed in the vast majority of ovarian carcinomas (see below).

Podocalyxin

Podocalyxin/PCLP-1/Thrombomucin/MEP21/gp135 and its close relatives endoglycan and CD34, belong to the CD34 family of cell surface sialomucins. These sialomucins have a conserved cytoplasmic tail with a C-terminal PDZ recognition site, a

single pass transmembrane region and a heavily glycosylated and sialylated extracellular domain that is bulky and negatively charged. Podocalyxin is normally expressed at the surface of vascular endothelia, mesothelial cells, hematopoietic progenitors, megakaryocytes, kidney podocytes, luminal breast epithelial cells, and a subset of neurons (Doyonnas et al., 2001; Kerjaschki et al., 1984; McNagny et al., 1997; Sassetti et al., 1998). Podocalyxin was originally identified as the major sialylated glycoprotein that contributes the majority of negative charge to human renal glomerular epithelial cells (podocytes) (Kerjaschki et al., 1984). Podocalyxin is specifically localized to the foot process of the podocyte (Sawada et al., 1986) where its high net negative charge maintains the filtration slits of the glomerular epithelium (Dekan et al., 1991). In glomerular epithelial development, podocalyxin expression by the typical polarized epithelium coincides with the basolateral descension of tight junctions and their modification into slit diaphragms (Schnabel et al., 1989). Loss-of-function studies have confirmed podocalyxin is indispensible for proper morphogenesis of the glomerular epithelium. Deletion of the podocalyxin gene in mice leads to anuria, omphalocephele, and perinatal lethality (Doyonnas et al., 2001). Strikingly, in the absence of podocalyxin, podocytes fail to form slit diaphragms and foot processes that allow the passage of the glomerular filtrate. This is associated with an aberrant maintenance of tight junctions and adherens junctions between affected podocytes (Doyonnas et al., 2001). Taken together, this evidence confirms that podocalyxin is required for proper morphogenesis of the glomerular epithelium and suggests that it may act as an anti-adhesin that alters cell junction dynamics.

Ectopic overexpression studies support podocalyxin's function as an anti-adhesin with cell-cell adhesion perturbing effects. Ectopic overexpression of podocalyxin in chinese hamster ovary (CHO) and MDCK cells caused an expression level dependent decrease in cell-cell aggregation, which was dependent on sialylation of podocalyxin's extracellular domain (Takeda et al., 2000). Overexpression of podocalyxin may also promote alterations that are associated with tumourigenesis. Using an outcome-linked breast tissue microarray, podocalyxin was found to be highly expressed in a subset of invasive carcinoma, where it served as an independent prognostic indicator of poor outcome (Somasiri et al., 2004). Furthermore, an analysis of podocalyxin expression in breast cancer cell lines revealed that podoclayxin was upregulated in highly metastatic cell lines. When podocalyxin was ectopically overexpressed in a well-differentiated breast cancer cell line, cell-cell interactions were perturbed. Ectopic podocalyxin was targeted specifically to the apical domain in monolayers, which displayed a bulging apical domain and were prone to delaminate from the monolayer. Altogether, this suggests that when podocalyxin is overexpressed during breast carcinogenesis it may act as an anti-adhesin with cell junction perturbing effects that are associated with an expansion of the apical domain (Somasiri et al., 2004).

Podocalyxin has also been described as an apical membrane protein required for correct apical-basal polarization. Recently, podocalyxin was identified as the human orthologue of canine gp135 (Meder et al., 2005), the prototypical apical membrane marker used for classic epithelial polarity studies (Ojakian and Schwimmer, 1988). In single MDCK cells attached to the substratum, podocalyxin localized to a pre-apical domain, thus exhibiting a polarized membrane distribution in the absence of cell-cell junctions. Interestingly, when podocalyxin was depleted from MDCK cells in collagen gels, they failed

to organize into polarized cysts (Meder et al., 2005). Thus, podocalyxin is an apical

membrane protein that may actually be required for apical-basal polarization in kidney

epithelial cells. Podocalyxin's hypothesized role as an apicalizing factor may rely on

proteins that regulate its apical localization and mediate the assembly of scaffolds that retain

apicalizing factors. This is evident in polarized MDCK monolayers where efficient apical

targetting of podocalyxin was suggested to rely on its ability to interact with NHERF-2

(Meder et al., 2005).

The sodium-proton exchange regulatory factor (NHERF) family of adaptor proteins is

comprised of NHERF-1/EBP-50, NHERF-2/E3KARP/TKA-1, which both serve as

intracellular binding partners for podocalxyin. NHERF-1 and NHERF-2 are closely related

and both consist of two tandem N-terminal PDZ domains and a C-terminal ezrin-binding

ERM domain. NHERF proteins bind the C-terminal PDZ recognition site of a variety of

membrane proteins, linking them to the actin cytoskeleton via interactions through their

ezrin-binding ERM domain, which in turn binds actin. NHERF binding partners include G-

protein coupled receptors and receptor tyrosine kinases, and receptors implicated in

regulating ion transport (Weinman, 2001). By mediating interactions with membrane

receptors and actin binding proteins, NHERF family proteins have been implicated in

stabilizing multiprotein complexes at the plasma membrane, as well as regulating ion

transport and signal transduction downstream of these receptors (Weinman et al., 2001).

The ability of NHERF-1 and 2 to bind the C-terminal DTHL motif of the podocalyxin

cytosolic tail (Li et al., 2002; Takeda et al., 2001; Tan et al., 2006) has been proposed to

mechanistically explain how NHERF/podocalyxin complexes promote the formation of

apical membrane domains (Meder et al., 2005). As they are PDZ-domain rich adaptor proteins, NHERFs are capable of mediating the assembly of multiprotein complexes linking podocalyxin indirectly to the actin cytoskeleton, through interactions with ezrin. NHERFs also may potentially localize podocalyxin to adherens junctions, either via putative interactions with β-catenin (Shibata et al., 2003), or via direct interactions with PTEN (Takahashi et al., 2006), which is recruited to adherens junctions during polarization by Par-3 (Pinal et al., 2006).

Podocalyxin's role in promoting apical membrane morphogenesis is further supported by evidence that its overexpression induces apical microvilli formation in both MDCK and breast cancer cells (Nielsen et al., 2005). Contrary to speculation in the field, the NHERF-binding PDZ recognition site was dispensible for microvilli formation, suggesting that apical targetting of podocalyxin occurs independently of NHERFs. In fact, induction of microvilli by podocalxyin only required the extracellular domain, transmembrane domain and six amino acids of cytoplasmic tail of podocalyxin. Therefore, NHERF's hypothetical role in regulating apical podocalyxin localization and stabilization requires further clarification. In contrast to these polarity-promoting roles, aberrant overexpression of podocalyxin during tumorigenesis may perturb cell adhesion, which is critical for apical-basal polarization.

Hypothesis:

The unique evolution of ovarian carcinoma suggests that alterations in cell polarity could play a role in driving the disease forward by modulating a number of important phenotypes that could include the early emergence of columnar metaplasia, the increased epithelial

differentiation during carcinoma formation, the decreased adhesion and effusion formation, and/or the adhesion to the peritoneal wall during secondary tumor formation. Given that podocalyxin appears to be an important modulator of epithelial polarity and the fact that I initially found that it is highly expressed in the majority of ovarian carcinomas, I predict that the molecule plays a role in the emergence of one or more of the above described phenotypes.

Objectives:

To assess whether podocalyxin is a prognostic indicator of outcome during ovarian carcinoma progression, podocalyxin expression was characterized in an outcome-linked ovarian tumour microarray (TMA) and a series of OSE-derived and ovarian carcinoma derived cell lines. To assess the functional role of podocalyxin in ovarian carcinoma, I ectopically overexpressed podocalyxin in a well-differentiated ovarian carcinoma cell line. Next, I subjected these cells to *in vitro* assays to assess the effects of podocalyxin overexpression on cell-cell aggregation, cell junction protein expression and localization and cell-ECM adhesion.

2. MATERIALS AND METHODS

Immunohistochemistry/Tissue Microarray

Formalin-fixed, paraffin-embedded specimens were sectioned into 5 μm slices on

Superfrost/plus slides (Fisher Scientific, Fair Lawn, NJ). After drying tissue overnight at

37°C, the sections were baked at 60°C for 1-2 hours and then cooled to room temperature.

The tissue sections were deparaffinized by incubating the slides 3 X 5 min in xylene. Tissue

sections were rehydrated with 2 X 3 min washes in absolute ethanol, followed by one 3 min

wash in 95% ethanol and finally with one 3 min wash in 80% ethanol. The tissue sections

were rinsed in a large volume of ddH$_2$0 for at least 2 minutes.

Antigen retrieval was performed using citrate buffer, pH 6.0 (18 ml of 0.1 M citrate acid in

82 ml of 0.1 M sodium citrate, up to 1 L with dH$_2$O), pre-heated to 90-98°C in a Coplin jar

incubated for 30 min in a steamer. Slides were incubated in the citrate buffer-filled Coplin

jar and steamed for 30 minutes. The Coplin jar was then removed from the steamer and

allowed to cool to room temperature for 20 minutes. The slides were rinsed with phosphate-

buffered saline (PBS), pH 7.4, 3 X 5 min.

Endogenous peroxide activity was blocked by incubating the sections with 3% hydrogen

peroxide for 10 minutes. The slides were rinsed 3 X 5 min with PBS and excess buffer was

blotted using a kimwipe. The primary antibody dilution was applied to the tissue and

incubated in a sealed immunochamber overnight at 4°C. To detect human podocalyxin,

monoclonal mouse podocalyxin 3D3 antibody (Kershaw et al., 1997) was diluted 1:1000 in

18

PBS. To detect human NHERF-1, rabbit anti-human NHERF-1 (AbCam, Cambridge, MA) was diluted 1:3000 in PBS.

Tissue sections were washed with PBS, 3 X 5 min. Secondary antibody conjugated to horseradish perodixidase (HRP)-labelled polymer (DAKO EnVision™+ System, Troy, MI) was applied to the tissue and incubated in a sealed immunochamber for 30 minutes at room temperature. Slides were washed 3 X 5 min with PBS.

Room temperature Nova Red™ reagents were prepared according to the manufacturer's protocol and applied to the tissue for approximately 3-5 minutes. Tissue sections were then rinsed 2 X 5 min with dH_2O and counterstained with Mayer's hematoxylin. The slides were washed with cold tap water for 10 minutes and dehydrated with 2 X 10 sec washes in 95% ethanol, 1 X 10 sec wash in absolute ethanol, 1 X 1 min wash in absolute ethanol. Finally, the sections were subjected to 2 X 3 sec xylene washes followed by one final 3 min xylene wash, after which the tissue was mounted using Permount (Fisher Scientific).

Cell culture

Established human ovarian carcinoma cell lines were routinely culture in a 1:1 mixture of 199/105 (Sigma, St. Louis, MO) supplemented with 5% fetal bovine serum (FBS, invitrogen, Carlsbad, CA) and 50 ug/ml Gentamycin Sulfate (Sigma) at 37°C in a 5% CO_2 humidified incubator. Transfected cell lines were maintained under selection using regular growth media supplemented with 400 µg/ml Geneticin (G418, Sigma).

Transfection

The pβ expression construct, which exhibits high levels of gene expression in mouse mammary epithelial EpH4 cells, was chosen for expression of mouse podocalyxin cDNA. This expresssion vector consists of the CMV IE enhancer/chicken β-actin promoter excised from pCAGGS with *Xho*I and *Eco*RI and cloned into a derivative of pcDNA3 (invitrogen) modified by the addition of an oligosaccharide linker (Pinkas and Leder, 2002). Mouse podocalyxin cDNA lacking its 3'-UTR was cloned into pβ vector to give pβ-podo. Cells were trypsinized one day prior to transfection. For stable transfection, cells were seeded at 30-40% confluency and transfected with 20 μg of DNA linearized with PvuI (invitrogen). Following DNA extraction, the pellet was resuspended in 20 μl ddH$_2$0 and added to 300 μl 199/105 rinse media. 15 μl DMRIE-C transfection reagent (invitrogen) was mixed with 300 μl 199/105 rinse media and added dropwise to the DNA mixture and mixed by bubbling. The transfection reagent was incubated for 20 min at room temperature. Cells were washed three times with 199/105 rinse media to remove traces of antibiotic. 2.4 ml of 199/105 supplemented with 2% FBS was added to the dishes and the transfection reagent was added dropwise to the plates and allowed to incubate for 6 hours. Plates were washed 3 times with 199/105 rinse media and cultured overnight in 5% FBS 199/105. The following day, cells were switched to normal growth serum. Two days following transfection, cells were placed under selection using normal growth media supplemented with 400 μg/ml G418 and selected for 14 days to generate heterogeneous populations of stable transfectants. OVCAR-3 and OVCAR-8 cells stably transfected with the empty pβ vector were designated OVCAR-3-vector and OVCAR-8-vector. OVCAR-3 and OVCAR-8 cells stably transfected with pβ-podo were designated OVCAR-3-podo and OVCAR-8-podo.

Fluorescence automated cell sorting (FACs)

After genetic selection, to enrich the population of OVCAR-3-podo and OVCAR-8-podo cells targetting mouse podocalyxin to the cell surface, cells were FAC sorted following indirect immunofluorescent labelling of mouse podocalyxin. OVCAR-3-vector and OVCAR-8-vector were used as a negative control and were collected by FACs to control for any phenotypic changes resulting from transfection and multiple FACs. Cells were trypsinized and resuspended in 1 ml FACs buffer (10% FBS, 0.025% sodium azide, filter sterilized PBS) and added to FACs tubes. Cells were centrifuged at 1000 rpm for 2 min and the supernatant was aspirated. Pellets were resuspended in 100 µl of a 1:50 dilution of rat anti-mouse PCLP-1 antibody (which recognizes an epitope in the extracellular domain of mouse, but not human, podocalyxin) (MBL, Nagoya, Japan) in FACs buffer and incubated on ice for 20 min. Cells were washed twice in 3 ml of FACs buffer. Pellets were then resuspended in 100 µl of a 1:250 dilution of biotinylated anti-rat IgM+IgG (H+L chain specific) (Southern Biotech, Birmingham, AL) in FACs buffer and incubated on ice for 20 min. Following two washes with FACs buffer, the pellet was resuspended in 100 µl of a 1:200 dilution of streptavidin-allophycocyanin (SAv-APC, BD Biosciences, San Jose, CA) and incubated on ice for 20 min in the dark. Following two washes with FACs buffer, cells were resuspended in 1 ml of FACs buffer. OVCAR-3-podo and OVCAR-8-podo were sorted for APC, thereby enriching for cells with high podocalyxin expression at their cell surface.

Matrigel™ basement membrane matrix (EHS)

Matrigel is a solubilized basement membrane isolated from Engelbreth-Holm-Swarm (EHS) mouse sarcoma, a tumour actively synthesizing extracellular matrix proteins (Kleinman et al.,

21

1982). Laminin is abundantly synthesized along with collagen IV, heparin sulfate

proteoglycans and entactin. Other constituents include TGF-β, fibroblast growth factor,

tissue plasminogen activator and other naturally occuring growth factors from the EHS

tumour.

Preparation of Matrigel^{TM} coated dishes and coverslips

Stocks of Matrigel were removed from -80°C and thawed overnight on ice at 4°C, and then

diluted 1:1 with cold 199/105 rinse media and kept on ice to prevent gelling. 12 well tissue

culture plates containing sterilized 18 mm coverslips were chilled at -20°C and placed on ice.

100 µl of diluted Matrigel was pipetted onto the centre of each coverslip using pre-chilled

200 µl pipette tips. The Matrigel was spread evenly upon each coverslip using the blunt end

of a 200 µl pipette tip and incubated at 37°C for 1 hr to allow gelling.

3D culture

Following trypsinization, cells were gently resuspended in 199/105 media supplemented with

2% FBS and 50 µg/ml gentamycin and seeded at 150 000 cells/ml. 1 ml of cell suspension

was plated onto each Matrigel-coated coverslip. Media was changed every other day. To

allow spheroid formation on gel, cells were cultured for five days, at which point they were

fixed in ice-cold methanol for 20 min at -20°C.

Whole cell lysis

10 cm dishes of confluent monolayers were rinsed three times with cold 199/105 base media

and then lysed in 300 µl of RIPA lysis buffer (150 mM NaCl, 50 mM Tris pH 7.4, 5 mM

EDTA, 5.0% NP-40, 1.0% sodium deoxycholate, and 0.1% sodium dodecyl sulphate, SDS) containing aprotinin, leupeptin, phenylmethyl-sulfonyl fluoride, pepA, EDTA, sodium vanadate, sodium fluoride. Dishes were scraped using a cell lifter and transferred to 1.5 ml centrifuge tubes on ice. Cells were incubated in lysis buffer on ice for 10 minutes and then centrifuged at 14, 000 rpm at 4°C for 15 min. Supernatants were collected and served as the whole cell lysate.

Cell fractionation lysis

Confluent monolayers in 10 cm dishes were rinsed three times with cold 199/105 base media. The soluble fractions were collected by lysing the cells in 300 μl CSK buffer (Hinck et al., 1994) (10mM PIPES pH 6.8, 50 mM NaCl, 300 mM sucrose, 3 mM MgCl$_2$, 0.5% Triton-X-100) containing the protease inhibitors previously mentioned. The dishes were incubated on ice for 20 min, periodically agitating the lysis buffer. Cells were scraped with a cell lifter and transfered to tubes and centrifuged at 14, 000 rpm for 10 min at 4°C. The supernatant was collected and served as the soluble cell fraction.

The pellet was lysed in 50 μl SDS-IP buffer (Hinck et al., 1994) (1% SDS, 2 mM EDTA in 10 mM Tris HCl pH 7.5) containing protease inhibitors and boiled for 10 min at 100°C. 100 μl CSK buffer was added to the tube and chilled on ice. The pellet was then subjected to 4 X 10 sec of sonication, cooling on ice in between each round of sonication. This portion of the lysate served as the cytoskeletal cell fraction.

Western blotting

For whole cell and fractionation lysates, protein concentrations were determined using Pierce

BCA protein assay kit (Pierce, Rockford, IL) according to the manufacturer's instructions.

When probing for podocalyxin, NHERF-1 or junctional proteins, 40 µg of protein was

separated by SDS-polyacrylamide gel electrophoresis (PAGE) gel and transferred to a

polyvinylidene fluoride (PVDF) membrane (Biorad, Hercules, CA).

Membranes were incubated with a blocking solution consisting of 5% skim milk powder

(SMP) in Tris (pH 7.5) buffered saline-Tween 20 (TBS-T) for 1 hr at room temperature,

followed by brief washing with TBS-T. Membranes were incubated with primary antibody

(prepared according to table below) overnight at 4°C.

primary antibody	company	dilution	dilution buffer
α-catenin ms anti-human	Transduction laboratories Mississauga, ON	1:250	1% BSA in TBS-T +NaAzide
β-catenin ms anti-human	Transduction laboratories Mississauga, ON	1:1000	1% BSA in TBS-T +NaAzide
E-cadherin ms anti-human	Transduction laboratories Mississauga, ON	1:2500	1% BSA in TBS-T +NaAzide
ERK 1/2	Santa Cruz biotechnology Santa Cruz, CA	1:2000	1% SMP in TBS-T
β1 integrin ms anti-human	Transduction laboratories Mississauga, ON	1:2500	1% BSA in TBS-T +NaAzide
Podocalyxin rat anti-mouse	R&D systems Minneapolis, MN	1:100	1% BSA in TBS-T +NaAzide
Podocalyxin (3D3) ms anti-human	gift (Kershaw et al., 1997)	1:1000	1% BSA in TBS-T + NaAzide
ZO-1 rb anti-human	Zymed laboratories San Francisco, CA	1:2500	1% BSA in TBS-T + NaAzide

Excess primary antibody was removed by washing the membranes 3 X 10 min with TBS-T. To detect the primary antibody, the membranes were incubated with HRP-conjugated goat anti-mouse, goat anti-rabbit, or goat anti-rat IgG (Jackson Immunoresearch, West Grove, PA) diluted 1:5000 in 1% bovine serum albumin (BSA, Fisher Scientific, Fair Lawn, NJ) in TBS-T for 1 hr at room temperature. Enhanced chemiluminescence reagents (ECL, Amersham, Arlington Heights, IL) were applied to detect the HRP signal following exposure of the membrane to Kodak X-OMAT film. A Kodak X-OMAT 2000A film processor was used to develop the film.

Immunocytochemistry and microscopy

For indirect immunofluorescence of ectopic mouse podocalyxin or junctional proteins, cells were fixed in ice-cold methanol for 20 min at -20°C. Coverslips were rehydrated with 3 X 5 min PBS (pH 7.4) washes. To block non-specific binding, coverslips were incubated for 30 min with 100 ul of blocking solution (10% normal goat serum (NGS, Jackson ImmunoResearch)/ 1% BSA in PBS) at room temperature. Coverslips were washed briefly in PBS and incubated with 60 μl of primary antibody dilution for 1 hr at room temperature. To wash away excess primary antibody, coverslips were washed four times in PBS with gentle shaking. To detect primary antibody binding, coverslips were incubated with 100 μl of secondary antibody dilution for one hour at room temperature. Following several washes with PBS, coverslips were incubated for 1.5 minutes with 100 μl of a 1:10,000 dilution of 4'6-Diamidino-2-phenylindole (DAPI, Sigma) in 1% BSA in PBS. Cells were washed 3 X 7 minutes with PBS while gently shaking and mounted with DABCO (95% glycerol, 2.5% 1,4-diazabicyclo[2.2.2]octane (DABCO, Sigma) in PBS) on glass slides.

Indirect immunofluorescence using cell monolayers cultured on 3 µm porous filter inserts was performed following the protocol for 18 mm glass coverslips, except for a few modifications. Each filter was incubated with 100 µl of primary and secondary antibody and subjected to extra washes to remove non-specific binding.

Imaging was performed using the 60X oil immersion objective of an Olympus FV1000 confocal microscope.

E-cadherin/ZO-1 dual staining

To dual stain for E-cadherin and ZO-1, coverslips were incubated in a primary antibody solution containing a 1:100 dilution of monoclonal mouse anti-human E-cadherin antibody (Transduction Laboratories) and a 1:100 dilution of polyclonal rabbit anti-human ZO-1 antibody (Zymed Laboratories) in 1% BSA in PBS. A secondary antibody dilution was prepared using a 1:100 dilution of Alexa Fluor 488 goat anti-mouse IgG (Molecular Probes, Eugene, OR) and a 1:100 dilution of Alexa Fluor 568 goat anti-rabbit IgG (Molecular Probes).

E-cadherin/podocalyxin dual staining

To dual stain for E-cadherin and podocalyxin, cells were incubated in a primary antibody solution containing a 1:100 dilution of monoclonal mouse anti-human E-cadherin antibody (Transduction laboratories) and a 1:100 dilution of rat anti-mouse podocalyxin antibody (R&D systems, Minneapolis, MN) in 1% BSA in PBS. The secondary antibody dilution was prepared using a 1:100 dilution of Alexa Fluor 488 goat anti-mouse highly cross-adsorbed

26

IgG (Molecular Probes) and a 1:100 dilution of Alexa Fluor 568 goat anti-rat IgG (Molecular Probes).

β-catenin/podocalyxin dual staining

To dual stain for β-catenin and podocalyxin, cells were incubated in a primary antibody solution containing a 1:100 dilution of monoclonal mouse anti-human β-catenin antibody (Transduction laboratories) and a 1:100 dilution of rat anti-mouse podocalyxin antibody (R&D systems) in 1% BSA in PBS. The secondary antibody dilution was prepared using a 1:100 dilution of Alexa Fluor 488 goat anti-mouse highly cross-adsorbed IgG (Molecular Probes) and a 1:100 dilution of Alexa Fluor 568 goat anti-rat IgG (Molecular Probes).

β1 integrin /podocalyxin dual staining

Dual staining for β1 integrin and podocalyxin was carried out by incubating filters with a primary antibody solution containing a 1:100 dilution of mouse anti-human β1 integrin antibody (R&D systems) and a 1:100 dilution of rat anti-mouse podocalyxin antibody (R&D systems) in 1% BSA in PBS. The secondary antibody dilution was prepared using a 1:100 dilution of Alexa Fluor 488 goat anti-mouse highly cross-adsorbed IgG (Molecular Probes) and a 1:100 dilution of Alexa Fluor 568 goat anti-rat IgG (Molecular Probes).

Adhesion assays
Cell-cell aggregation assay (Hanging Drop)

Since cell-cell aggregation relies on intact cell surface molecules, cells were removed from the tissue culture dish without trypsinization. Cells were treated with 3 X 20 min calcium-

free media washes and then incubated with 2 ml enzyme-free cell dissociation buffer (invitrogen) for about 20 min or until the cells detached from the dish. Cells were resuspended at 1×10^6 cells/ml in normal growth media. 30 µl of the cell suspension was plated in droplets on the underside of a 24 well plate lid, corresponding to the centre of each well. The lid was replaced on the bottom of the plate, with the wells underneath the hanging droplets filled with sterile PBS. Hanging droplets were incubated for 24 hrs to allow cell aggregation to occur. Cell clusters were imaged by phase-contrast microscopy using the 10X objective and images were collected by a Nikon Coolpix camera.

Cell-ECM adhesion assay

Substrates for assaying cell adhesion were prepared in triplicate wells in a 96-well plate for each timepoint analyzed. 50 µl of 25 µg/ml bovine serum fibronectin in sterile PBS was plated in a 96-well plate and allowed to attach overnight at 4°C. 50 µl of 10 µg/ml or 20 µg/ml anti-β1 integrin antibody in sterile PBS was plated in a 96-well plate and allowed to attach overnight at 4°C. Fibronectin and β1 integrin antibody-coated wells were blocked with adhesion assay buffer (Dulbecco's modified Eagle's media (DMEM) calcium-free base media supplemented with 2 mM $CaCl_2$, 0.1% BSA) for 1 hr prior to plating cells. Negative control wells containing 100 µl of 1% BSA in PBS were plated in triplicate for each time point and incubated at 37°C for 2 hr prior to plating cells. To assay cell adhesion to mesolthelial cell monolayers, 30, 000 HUITLP9 cells were plated on 5 µg/ml bovine serum fibronectin in a 96-well plate and cultured for 48 hrs until they formed a fully confluent monolayer.

Cells were removed from the dish as previously described with enzyme-free cell dissociation buffer. Cells were resuspended at 5 X 10^5 cells/ml in adhesion assay buffer. The cell suspension was labelled with 25 μM 5-chloromethylfluorescein diacetate (CMFDA, Molecular Probes) for 30 min at 37°C. Cells were pelleted at 1000 g for 4 min and resuspended in adhesion assay buffer and incubated for another 30 min at 37°C. Cells were pelleted, resuspended in fresh adhesion assay buffer and plated in triplicate into wells containing substrate. After incubating cells at 37°C to allow attachment to occur, a fluorescent reading was taken of the 96-well plate to determine the total fluorescence emission for the total cells plated. Fluorescence emission was quantified using a fluorescence plate reader with filters set for absorption/emission at 485/530 nm. Following four washes with adhesion assay buffer, fluorescence emission was quantified for the remaining adherent cells. Percent adhesion was calculated by dividing the fluorescence emission of adherent cells by total fluorescence emission of plated cells (X100).

Enzyme-treatment was performed on cell suspensions that had been labelled with CMFDA and subjected to one 30 min wash. The cell suspension in adhesion assay buffer was treated with 250 mU/ml Neuraminidase or 0.2 μg/μl O-sialoglycoprotein endopeptidase and incubated for 45 min at 37°C. Cells were resuspended and 50 μl of cell suspension containing enzyme was plated into fibronectin-coated wells and assayed as previously described. 2.5 X 10^5 OVCAR-3-vector and OVCAR-3-podo cells were either treated with 250 mU/ml Neuraminidase or 0.2 μg/μl O-sialoglycoprotein endopeptidase or untreated for 45 min at 37°C and then pelleted and lysed in 30 μl RIPA buffer containing protease

inhibitors and subjected to Western blot analysis for mouse podocalyxin to verify that the enzymatic treatments had successfully altered the mouse podocalyxin ectodomain.

FBS dialysis

FBS was dialyzed to remove divalent cations by incubating FBS in dialysis tubing and stirring in 2 L of Tris (pH 7.5) NaCl buffer at 4°C for five days. Buffer was replaced every 24 hrs.

Calcium switch cell-cell adhesion assay

Cells were cultured under normal growth conditions on 3 μm porous filters until fully confluent. Calcium was depleted from culture conditions by washing three times with calcium-free DMEM base media and replacing with low calcium media (LCM), containing 5% dialyzed FBS, 5 μM $CaCl_2$ in calcium-free DMEM base media. Cell monolayers were incubated in LCM for 3-5 hrs to disassemble adherens junctions. LCM was removed and replaced by high calcium media (HCM), which consisted of normal growth media (1.8 mM $CaCl_2$). At the chosen time points, media was removed from the filter and the cells were fixed in ice-cold methanol at -20°C for 15 min.

Single cell attachment assay

Cells were treated with 3 X 20 min calcium-free media washes and then incubated with 2 ml enzyme-free cell dissociation buffer (invitrogen) for about 20 min or until cells detached from the dish. To ensure that cell surface proteins are intact, this tryspin-free method ensures that podocalyxin and other cell surface molecules will not by proteolytically cleaved.

Cells were seeded at 2.5×10^5 cells/ml onto sterilized 18 mm glass coverslips and incubated for 4 hrs, at which point they were fixed in ice-cold methanol at $-20°C$ for 20 min.

3. RESULTS

Analysis of podocalyxin expression in ovarian carcinoma and the normal ovary

Podocalyxin has been described as an independent prognostic indicator of poor outcome during breast cancer progression (Somasiri et al., 2004). Overexpression of podocalyxin was detected in a small subset of invasive breast carcinomas present on a breast tissue microarray and correlated with a decrease in disease-specific survival. Since ovarian cancer and breast cancer exhibit many common genetic and epigenetic changes (Roskelley and Bissell, 2002), we investigated whether the features of podocalyxin overexpression in breast cancer also applied to ovarian cancer. Immunohistochemical analysis of podocalyxin expression was carried out on an ovarian tumour microarray (TMA) containing 529 outcome-linked specimens. Each specimen was scored 0 for podocalyxin negative, or 1 for low podocalyxin expression, or 2 for high podocalyxin expression. For the purposes of the outcome-data analysis, low and high podocalyxin expression were grouped in the same category as podocalyxin positive (score 1). One of the most striking characteristics of the ovarian TMA was that, in contrast to the breast TMA, the overwhelming majority of tumour specimens were podocalyxin positive (84.88%) (Fig. 1A). Two well-represented histological tumour subtypes on the array, serous and mucinous, were 96% and 90% positive for podocalyxin expression, respectively (Fig. 1B). Despite the prevalence of podocalyxin expression in epithelial ovarian cancer, Kaplan-Meier analysis of disease-specific survival (log-rank test) indicated that, while there was a slight trend, podocalyxin expression is not associated with poor outcome in a statistically significant manner (P=0.5793) (Fig. 1A). Interestingly, podocalyxin expression may only have prognostic value among tumours of a

Figure 1. Analysis of podocalyxin expression in an outcome-linked ovarian tumour microarray.

Using tumour microarray (TMA) technology, immunohistochemical staining for podocalyxin was performed on 529 outcome-linked ovarian carcinoma specimens.

A) Survival plot for podocalyxin negative (score 0) or podocalyxin positive (score 1) groups showed no significant correlation between podocalxyin expression and patient outcome. Kaplan-Meier analysis (log rank test) revealed no significant difference in disease-specific survival between group 0 and group 1 (P=0.5793).

B) Table representing the distribution of podocalyxin negative (score 0) and podocalyxin positive (score 1) lesions among ovarian tumours of various histological subtypes.

A
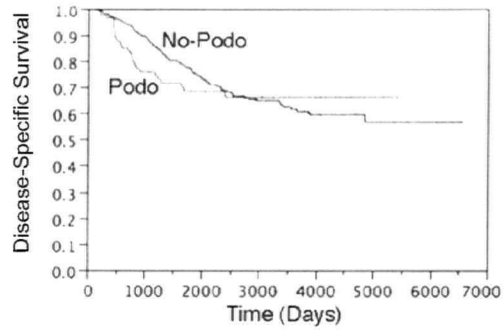
B

primary cell type total %	score 0	score 1	total specimens
adenocarcinoma NOS	0 0.00	3 0.57	3 0.57
clear cell	48 9.07	92 17.39	140 26.47
endometriod	13 2.46	117 22.12	130 24.57
mucinous	7 1.32	27 5.10	34 6.43
serous	8 1.51	199 37.62	207 39.13
squamous cell	0 0.00	1 0.19	1 0.19
transitional	1 0.19	6 1.13	7 1.32
undifferentiated	3 0.57	4 0.76	7 1.32
total total %	80 15.12	449 84.88	529

specific histological subtype. For example, podocalyxin positive tumours classified as clear cell carcinoma, 66% scored 1, compared to 96% of serous carcinoma which scored 1 (Fig. 1B).

The majority of epithelial ovarian carcinomas are currently thought to arise from the OSE. To investigate whether podocalyxin and its binding partner NHERF-1 are expressed in the proposed precursor to ovarian carcinoma, immunohistochemistry for podocalyxin and NHERF-1 expression was performed on normal human ovary. In the normal ovary, podocalyxin and NHERF-1 expression was moderate and highly specific to normal OSE, serving to distinguish the OSE from its underlying stroma (Fig. 2). Podocalyxin localizes to the free peritoneal surface, whereas NHERF-1 is somewhat less restricted in its localization. Podocalyxin and NHERF-1 staining was absent in the cells of the underlying stroma, however, deeper into the vascularized regions of the ovarian cortex, vascular endothelial cells were highly positive for podocalyxin staining. Vascular endothelia have been widely characterized as podocalyxin positive (Horvat et al., 1986), thus serving as an internal control verifying the specificity of the podocalyxin antibody. Podocalyxin and NHERF-1 expression is also highly specific to OSE lining dysplastic surface clefts. Interestingly, podocalyxin was apically localized in dysplastic, columnar OSE, thus emphasizing that it may serve as a marker of polarity early in carcinogenesis (Fig. 2). Consistent with this observation was the apical localization of podocalyxin in many low-grade well-differentiated tumours (Fig. 3 C, E, G). This suggests that, in addition to kidney epithelial cells (Meder et al., 2005), podocalyxin is as an apical membrane marker in polarized ovarian carcinoma cells. Furthermore, since assymetrical podocalyxin localization is a feature of polarized cells,

35

Figure 2. Podocalyxin and NHERF-1 are expressed in the ovarian surface epithelium and epithelia of the female reproductive tract.

Immunohistochemical analysis for podocalyxin and NHERF-1 was performed on formalin fixed, paraffin-embedded human ovary, oviduct and endometrium specimens. (Scale bar = 0.3 mm).

	podocalyxin	**NHERF-1**

OSE
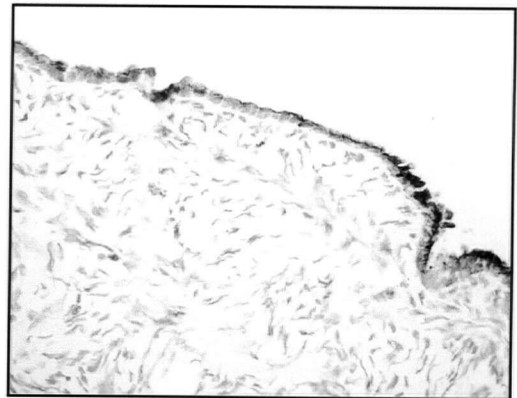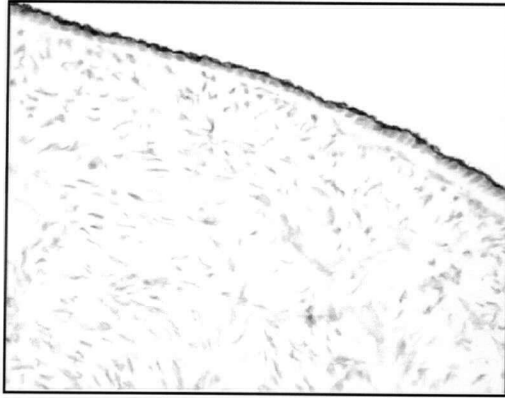
surface
cleft
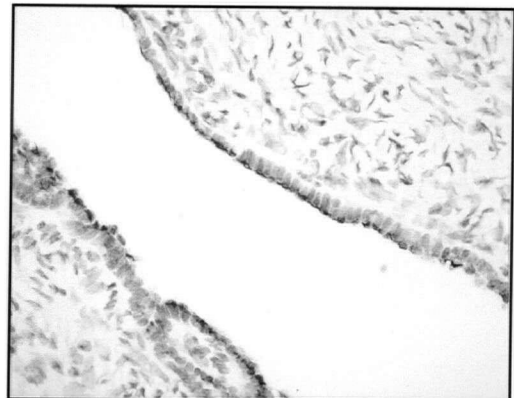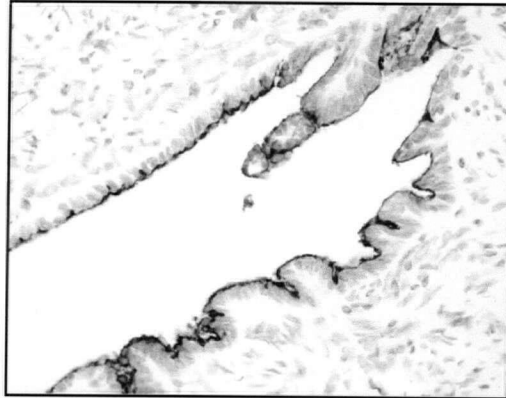
oviduct
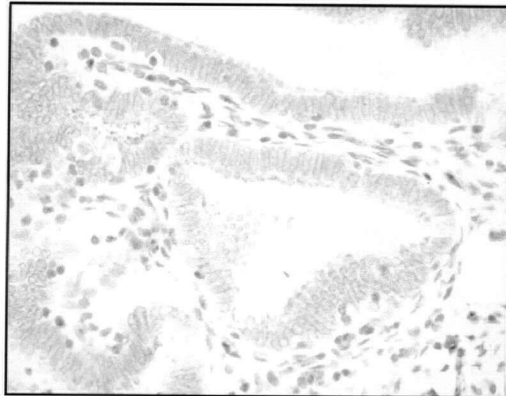
endo-
metrium
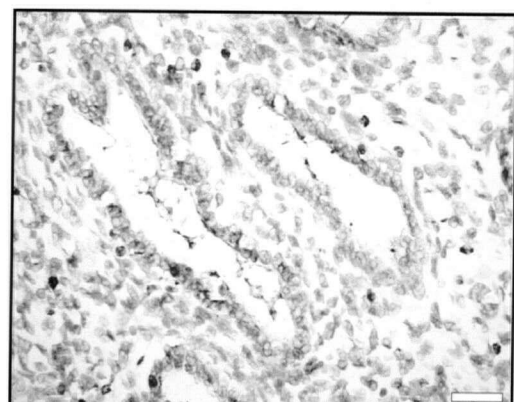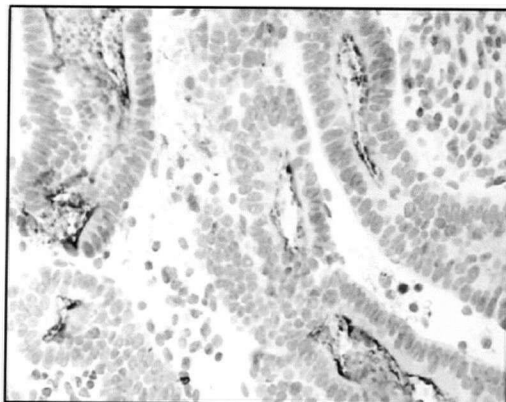
Figure 3. Ovarian TMA specimens exhibit two distinct patterns of podocalyxin localization.

Immunohistochemical analysis of podocalyxin expression in an outcome-linked ovarian TMA revealed two distinct patterns of podocalyxin localization: polar and non-polar.

A) A podocalyxin negative ovarian carcinoma exhibited positive staining for podocalyxin in vascular endothelia only.

B), D), F), H) provide examples of non-polar podocalyxin localization in tumours ranging from very low to high levels of podocalyxin expression.

C), E), G) provide examples of apically restricted, polarized podocalyxin localization in tumours with increasing levels of podocalyxin expression. (Scale bar = 0.5 mm).
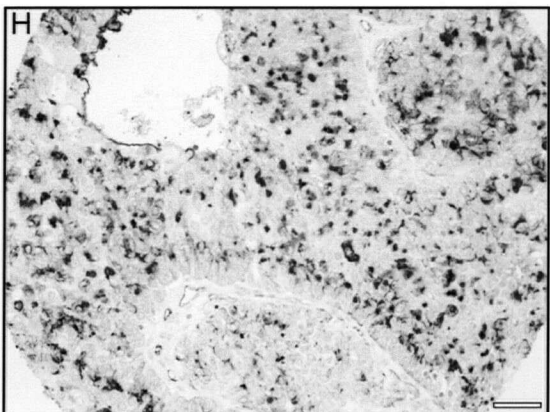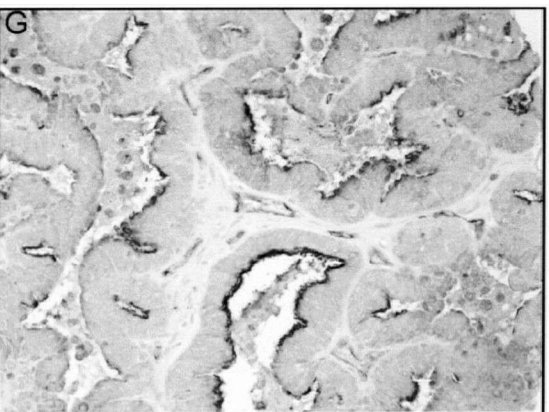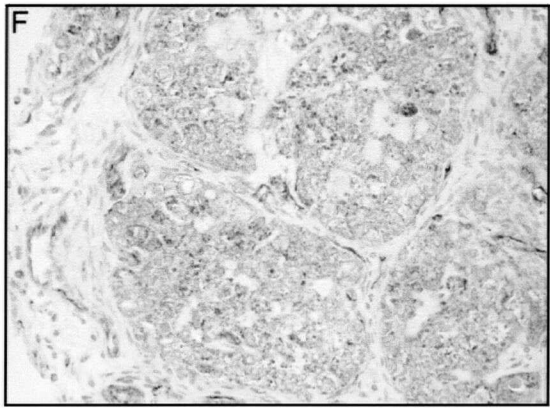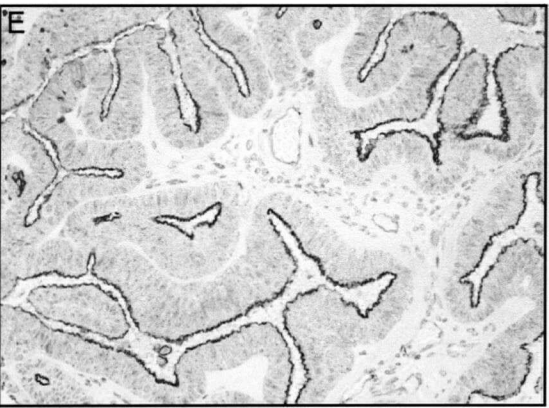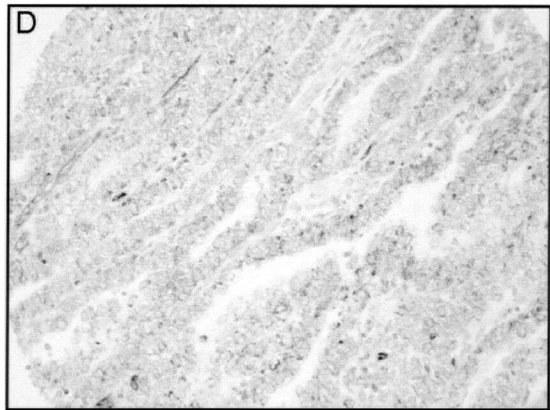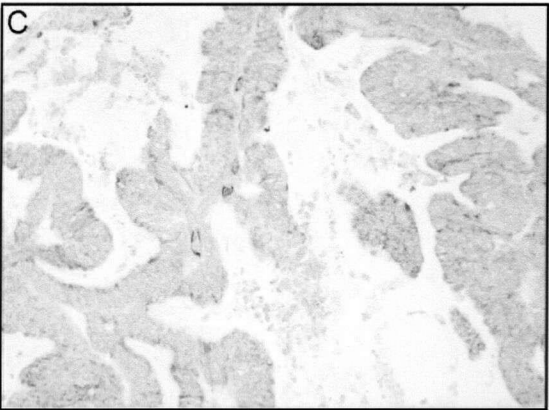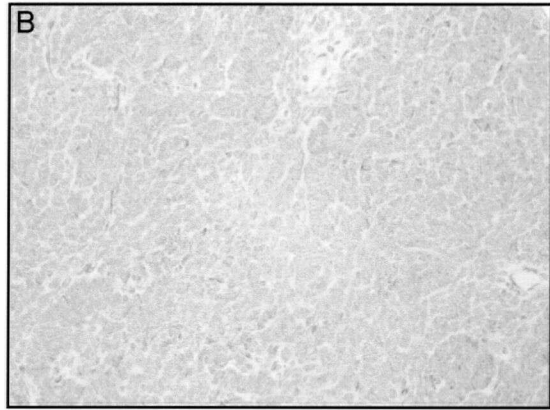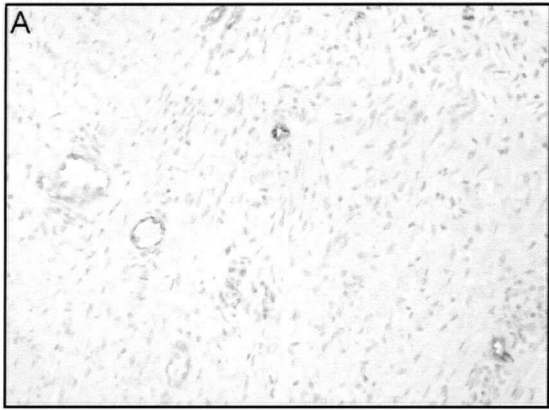
podocalyxin also serves as a marker of cell polarity in ovarian tumours, which may be useful for helping to assign tumour grade.

The Mullerian duct-derived epithelia of the oviduct and endometrium share a common embryonic precursor with the OSE, the coelomic epithelium. This relationship is evident among well-differentiated ovarian carcinomas, which are classified into histological subtypes according to their morphological resemblance to these epithelia (Barber, 1993). The normal Mullerian duct-derived epithelia of the endometrium and oviduct assumed a columnar morphology, allowing podocalyxin localization at the apical domain to be discerned. Apical to podocalyxin expressing cells, the glandular lumina of the endometrium stained positively for podocalyxin, implying that podocalyxin may be shed from the apical membrane. In addition, some highly polarized podocalyxin positive ovarian tumours from the TMA exhibited podocalyxin staining in the apical extracellular space (Fig. 3G). Therefore, podocalyxin may be shed from the apical membrane in certain ovarian carcinomas. Ovarian TMA analysis confirmed that podocalyxin is widely expressed among primary ovarian carcinomas as well as the proposed cell of origin for ovarian carcinoma, the OSE.

Previously, characterization of breast carcinoma cell lines revealed that high podocalyxin expression correlates with increased invasive potential (Somasiri et al., 2004). Given this potential association, I first sought to characterize whether podocalyxin expression correlates with cell junction integrity in a series of human ovarian cells lines, derived either from the OSE or from morphologically distinct human ovarian carcinomas. This also

allowed me to select an appropriate cell line in which to carry out ectopic podocalyxin overexpression studies.

Junctional properties and podocalyxin expression in OSE-derived and ovarian carcinoma cell lines

In order to evaluate cell junction complex formation in the cell lines surveyed, markers of adherens junctions and tight junctions were assessed for expression and localization. E-cadherin was selected as a marker for adherens junctions, while ZO-1 served as a marker for tight junctions. Western blot analysis for E-cadherin and ZO-1 was performed using whole cell lysates prepared from IOSE-80pc, an immortalized human OSE-derived cell line, along with a series of ovarian carcinoma-derived cell lines, A2780, OVCAR-10, CaOV-3, OVCAR-3, OVCAR-8 and SKOV-3 (Fig. 4). MDA-231 and T47D are breast carcinoma-derived cells lines that were used as an E-cadherin negative and positive control, respectively. IOSE-80pc displayed a fibroblastic, migratory morphology in culture (not shown), which is reminiscent of the phenotype assumed by OSE cells when they undergo wound repair *in vivo*. E-cadherin was not expressed by IOSE-80pc, a characteristic of the OSE retained by this cell line. Similarly, the A2780 and OVCAR-10 cell lines did not express E-cadherin. The highly differentiated ovarian carcinoma cell lines CaOV-3, OVCAR-3 and OVCAR-8 displayed a cobblestone morphology in monolayer culture (not shown). These cell lines all expressed E-cadherin, which is generally considered a characteristic of well-differentiated tumours (Davidson et al., 2000; Davies et al., 1998; Hough et al., 2000; Sundfeldt et al., 2001; Sundfeldt et al., 1997). The highly invasive de-

Figure 4. Podocalyxin and NHERF-1 expression in OSE-derived and ovarian carcinoma-derived cell lines.

Whole cell lysates were prepared from IOSE-80pc, an immortalized human OSE-derived cell line, along with a series of ovarian carcinoma-derived cell lines, A2780, OVCAR-10, CaOV-3, OVCAR-3, OVCAR-8 and SKOV-3. MDA-231 and T47D breast cancer cells lines were used as a podocalyxin positive and negative control, respectively (Somasiri et al., 2004). 40 µg of whole cell lysate was resolved by SDS-PAGE and analyzed by Western blotting using antibodies against E-cadherin, ZO-1, NHERF-1 and podocalyxin.

149

36 50

149 250

98 149 250

IOSE-80pc

A2780

OVCAR-10

CaOV-3

OVCAR-3

OVCAR-8

SKOV-3

T47D

MDA-231

podocalyxin (140 kDa)

NHERF-1 (50 kDa)

ZO-1 (225 kDa)

E-cadherin (120 kDa)

43
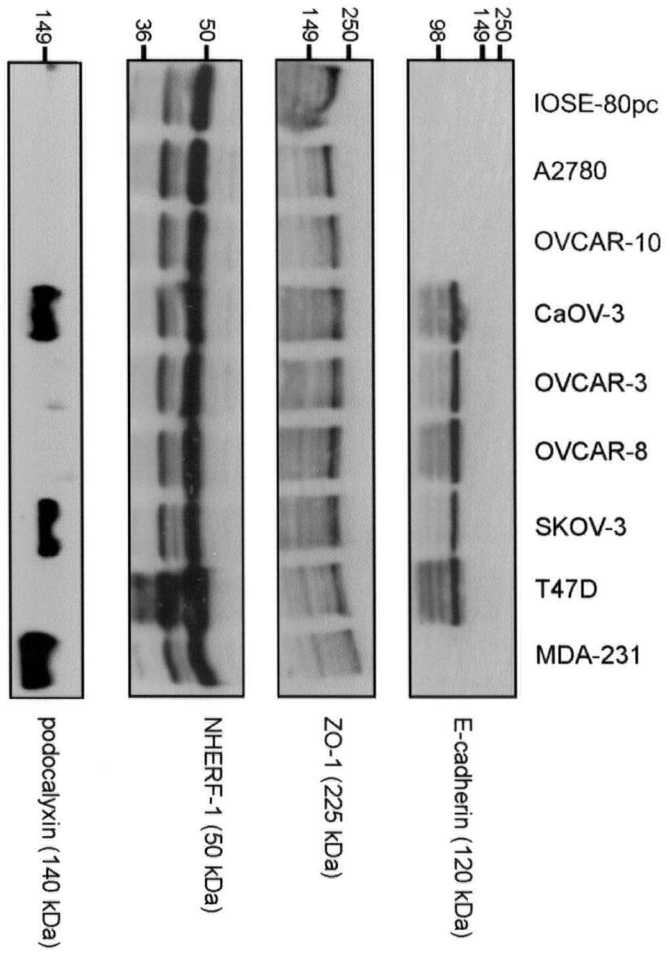
differentiated ovarian carcinoma cell line SKOV-3 also expressed some E-cadherin although it was less than that observed in most of the differentiated lines. ZO-1 expression was similar among all the cell lines, thus ZO-1 expression did not correlate with a differentiated morphology. In order to characterize cell junction formation in these cell lines, the localization of adherens junction and tight junction marker proteins was next assessed by immunofluorescence.

Dual immunofluorescence staining for E-cadherin and ZO-1 was performed to assess adherens and tight junction protein localization, respectively (Fig. 5). The immortalized OSE-derived cell line, IOSE-80pc, which did not express E-cadherin, did not assemble extensive cell junctions based on the diffuse, cytoplasmic ZO-1 localization. A2780 and OVCAR-10 did not express E-cadherin by Western analysis, but did exhibit some background cytoplasmic staining. A2780 localized ZO-1 diffusely in the cytoplasm, suggesting that this cell line did not assemble cell junction complexes. OVCAR-10, despite the absence of E-cadherin, did exhibit some discontinuous ZO-1 puncta at cell borders. E-cadherin and ZO-1 staining was localized to points of cell-cell contact in CaOV3 cells, which in the merged field appear to exhibit some colocalization. OVCAR-3 and OVCAR-8 displayed similar junctional characteristics, with both E-cadherin and ZO-1 localizing continuously to points of cell-cell contact. SKOV-3 cells localized limited amounts of E-cadherin as well as ZO-1 continuously to cell-cell contacts in confluent regions of the monolayers. In other less confluent regions, E-cadherin is predominantly cytoplasmic and only small puncta of ZO-1 localized to cell contacts. Overall, the immunolocalization of E-cadherin and ZO-1 suggested that OVCAR-3, OVCAR-8 and CaOV3 displayed well-defined

44

Figure 5. Characterization of cell junction protein localization in OSE-derived and ovarian carcinoma cell lines.

Dual immunofluorescent staining for E-cadherin, a marker of adherens junctions, and ZO-1, a marker of tight junctions, was performed on IOSE-80pc, an immortalized human OSE-derived cell line, and a series of ovarian carcinoma cell lines including A2780, OVCAR-10, CaOV-3, OVCAR-3, OVCAR-8 and SKOV-3. Images shown are confocal projections of xy slices (Scale bar = 10 μm).

E-cad ZO-1 E-cad/ZO-1

IOSE-80pc

A2780

OVCAR-10

OVCAR-3

OVCAR-8

CaOV-3
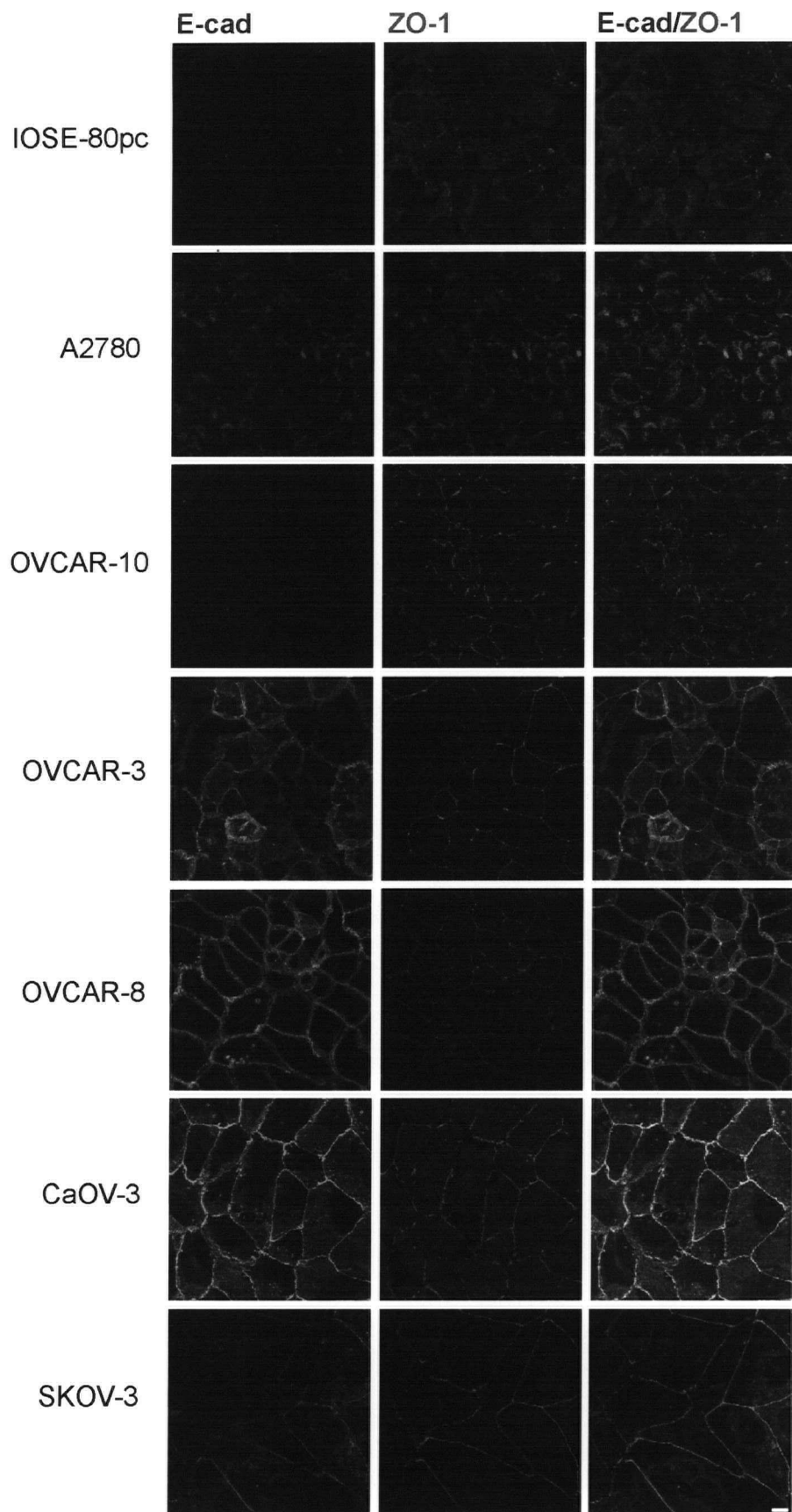
SKOV-3

junctional characteristics. The other cell lines OVCAR-10 and SKOV-3 displayed an intermediate junctional phenotype with some partial assembly of junctional complexes, whereas IOSE-80pc and A2780 did not assemble cell junctional complexes.

To determine whether podocalyxin expression displays an inverse correlation with well-defined cell junctions, podocalyxin expression levels were assessed in these OSE-derived and ovarian carcinoma-derived cell lines. Endogenous podocalyxin expression varied among cell lines and in most cases high podocalyxin expression was a feature of cell lines with poorly defined cell junctions. For example, SKOV-3, which did not assemble extensive cell junctions, expressed the highest levels of podocalyxin. The differentiated ovarian carcinoma cell lines OVCAR-3 and OVCAR-8 exhibited low podocalyxin expression. CaOV-3 provided an exception to this general trend since this cell line localized E-cadherin and ZO-1 to cell contacts yet was found to express very high levels of podocalyxin by Western blot analysis. Thus, in spite of the general trend observed between high podocalyxin expression and poorly defined cell junctions, it could not be absolutely concluded that these two factors are associated. Western blot analysis of the cytosolic podocalyxin binding partner NHERF-1 revealed that its expression was similar among these cell lines (Fig. 4).

Ectopic overexpression of mouse podocalyxin in human ovarian carcinoma cells

To test my hypothesis that high podocalyxin expression contributes to disruption of cell polarity and/or adhesion during ovarian cancer progression, I chose to overexpress podocalyxin in two ovarian carcinoma cell lines, OVCAR-3 and OVCAR-8, with low

endogenous podocalyxin and well-differentiated junctional characteristics. As there is no appropriate antibody for immunofluorescent staining of human podocalyxin and because the use of an epitope tag to detect the protein may disrupt its function, the mouse podocalyxin cDNA was chosen for ectopic expression. Detection of mouse podocalyxin was then achieved with a species-specific antibody. Expression of mouse podocalyxin was highly inefficient in stably transfected cell populations (OVCAR-3-podo and OVCAR-8-podo). In order to enrich for ectopically overexpressed mouse podocalyxin, FACs was performed for fluorescently labelled mouse podocalyxin at the cell surface. Immunofluorescent staining of ectopic podocalyxin expression in single FAC sorted OVCAR-8-podo monolayers revealed that mouse podocalyxin expression was still quite heterogeneous and it was not targetted well to the apical membrane and was instead mostly diffuse and cytoplasmic (Fig. 6). Since podocalyxin was not efficiently targetted to the appropriate membrane domain, OVCAR-8-podo cells were not used further to assess the functional consequences of podocalyxin overexpression.

After three successive rounds of FACs, ectopic podocalyxin overexpression was achieved in the great majority of the OVCAR-3-podo population (Fig. 6). The presence of the protein was confirmed by Western blotting (see Fig. 9 below). OVCAR-3-vector cells were subjected to the same procedure to control for phenotypic effects resulting from the FACs procedure. Ectopic podocalyxin was targetted appropriately to the apical domain in OVCAR-3-podo (Fig. 6). Therefore, FACs enriched OVCAR-3-podo cells were used to perform a variety of *in vitro* assays to assess the phenotypic consequences of podocalyxin overexpression.

Figure 6. Characterization of E-cadherin, ZO-1 and mouse podocalyxin localization in well-differentiated ovarian carcinoma cells ectopically overexpressing mouse podocalyxin.

Confluent monolayers of OVCAR-3-vector, OVCAR-3-podo, OVCAR-8-vector and OVCAR-8-podo cells on coverslips were fixed and dual immunostained for E-cadherin/mouse podocalyxin or ZO-1/mouse podocalyxin. Podocalyxin immunostaining was performed to assess the percentage of podocalyxin positive cells in the population after expansion following FACs to enrich for podocalyxin expression at the cell surface. E-cadherin and ZO-1 immunostaining was performed to assess whether podocalyxin overexpression disrupted cell junction protein localization.

A) OVCAR-3 vector and OVCAR-3 podo underwent three successive FAC sorts

B) OVCAR-8-vector and OVCAR-8-podo cells underwent one FAC sort. Confocal projections of xy slices are shown with a corresponding z section. (Scale bar = 10 μm).

A

OVCAR-3-vector

E-cad/podo

OVCAR-3-podo

E-cad podo E-cad/podo

ZO-1/podo ZO-1 podo ZO-1/podo

B

OVCAR-8-vector

E-cad/podo

OVCAR-8-podo

E-cad podo E-cad/podo

ZO-1/podo ZO-1 podo ZO-1/podo
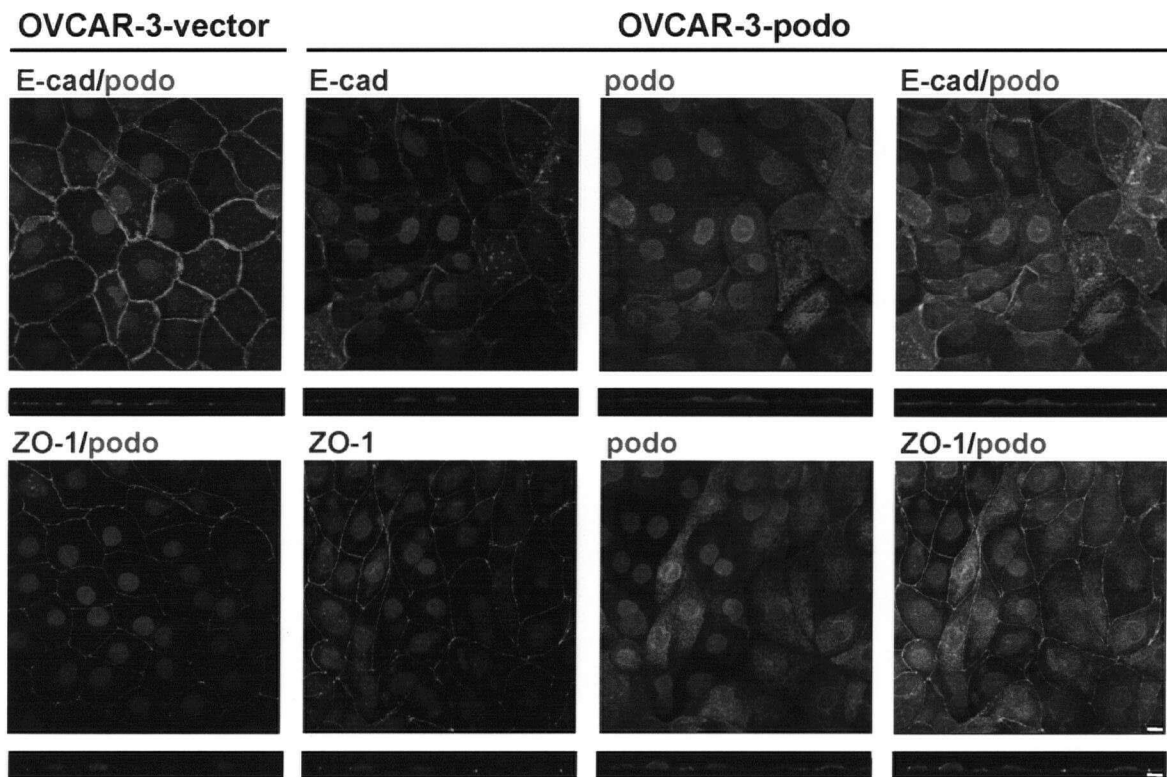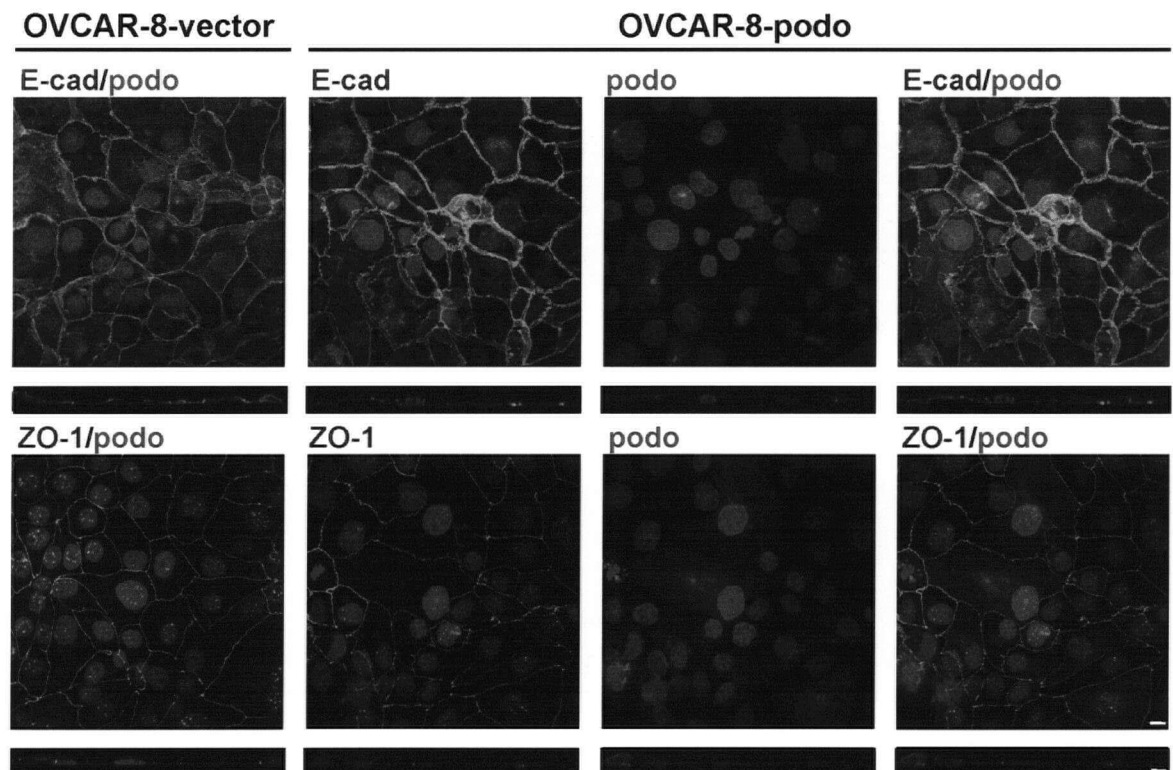
Podocalyxin overexpression inhibits OVCAR-3 cell-cell aggregation

Overexpression studies using chinese hamster ovary (CHO) and MDCK dog kidney

cells have established that podocalyxin disrupts cell-cell aggregation in an expression level-

dependent manner (Takeda et al., 2000). To determine whether podocalyxin overexpression

disrupts cell adhesion in ovarian carcinoma cells, cell-cell aggregation of OVCAR-3-podo

cells was assessed using a stationary hanging drop cell aggregation assay. This assay was

chosen because other assays such as the type performed by Takeda et al. with MDCK cells

employ shaking for the duration of the assay which, in the case of OVCAR-3 cells,

completely abolishes cell-cell aggregation. In the hanging drop assay, podocalyxin

overexpression in OVCAR-3 cells clearly inhibited the formation of cohesive cell aggregates

(Fig. 7). As a result, the majority of OVCAR-3-podo cells were present as single suspended

cells, whereas the OVCAR-3-vector cells formed large, irregular shaped clusters.

Podocalyxin's highly negatively charged extracellular domain has been shown to

mediate its anti-adhesive effects in MDCK cells (Takeda et al., 2000). To confirm that the

disrupted cell aggregation in OVCAR-3-podo cells was mediated by podocalyxin's

ectodomain suspended cells were subjected to enzymatic treatment to cleave the podocalyxin

ectodomain (Fig. 7). O-sialoglycoprotein endopeptidase is a metalloprotease that specifically

cleaves proteins that are O-glycosylated on serine and threonine residues (Abdullah et al.,

1992). Therefore, O-sialoglycoprotein endopeptidase cleaves a variety of O-

sialoglycoproteins and sulfated glycoproteins including CD34, CD43 and CD44 (Sutherland

et al., 1992). Western blot analysis for mouse podocalyxin in OVCAR-3-podo cells

subjected to endopeptidase treatment revealed a very faint band at approximately 140 kDa.

Figure 7. Podocalyxin overexpression disrupts the formation of cohesive cell clusters in suspension.

Cell aggregation was assessed using a hanging drop cell-cell adhesion assay. 1×10^6 cells/ml of OVCAR-3-vector and OVCAR-3-podo cells were cultured in a 30 µl suspended droplet overnight and imaged by phase-contrast microscopy using the 10X objective. Cell suspensions were either untreated or were treated just prior to plating with O-sialoglycoprotein endopeptidase (0.2 µg/µl), which cleaves podocalyxin's extracellular domain. Images of untreated cell droplets are representative of three independent experiments. Images of endopeptidase treated cells are representative of four replicates.

	OVCAR-3-vector	**OVCAR-3-podo**
untreated		
endo-peptidase		
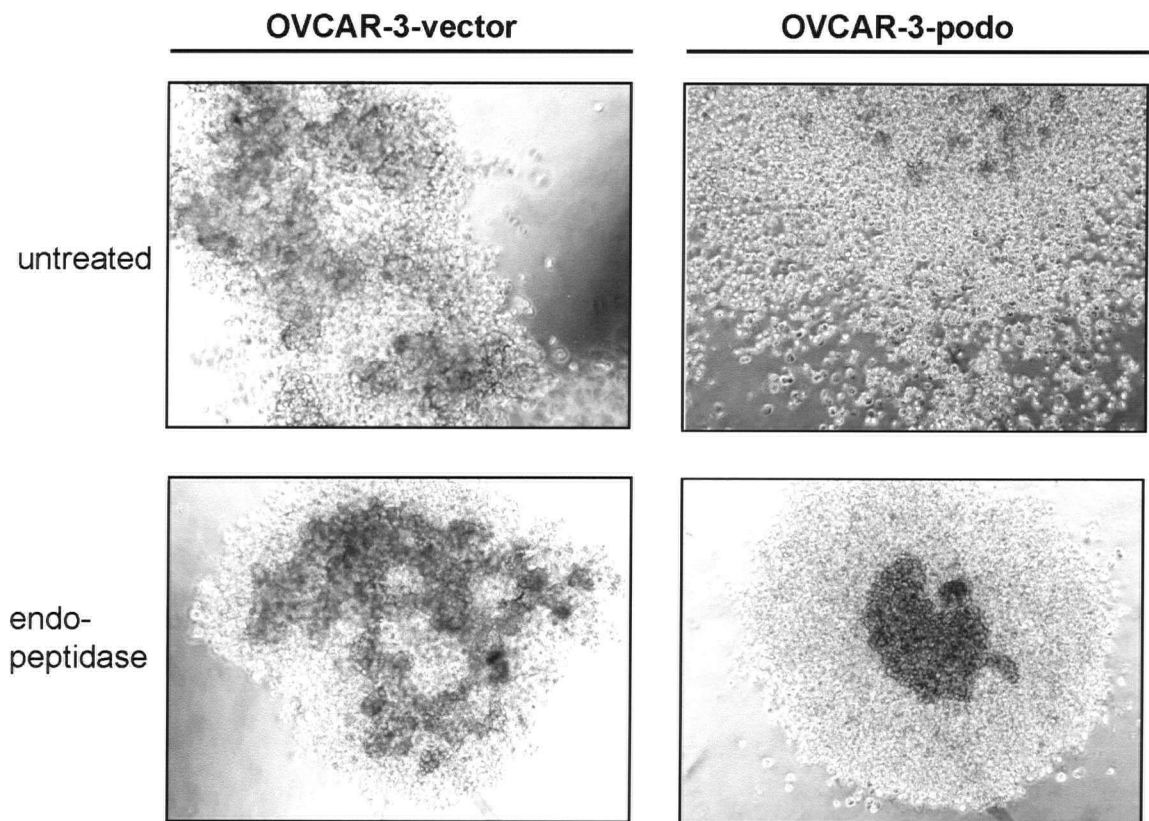
Complete enzymatic cleavage would have resulted in the complete absence of a band since

this antibody recognizes the mouse podocalyxin ectodomain (Fig. 13B). Untreated OVCAR-

3-vector cells formed loose irregular clusters, whereas endopeptidase treated OVCAR-3-

vector cells formed a single cohesive cluster. Clearly, cleavage of other glycoproteins

besides podocalyxin promoted cell aggregation in the vector control. Meanwhile,

endopeptidase treatment of OVCAR-3-podo cells caused a complete reversal of the anti-

adhesive podocalyxin phenotype, yielding a single compact spheroid, with few stray

suspended cells. Although cleavage of other glycoproteins besides podocalyxin must have

contributed to this reversal, endopeptidase treatment of OVCAR-3-podo cells resulted in a

more dramatic phenotypic shift than in the vector controls, going from single cells to one

cohesive spherical cluster following enzyme treatment. This shift was very consistent and

happened in all four replicates of the hanging drop clusters. Therefore, it can be concluded

that the podocalyxin ectodomain contributes to disaggregation of suspended clusters of

OVCAR-3-podo cells. Since podocalyxin overexpression disrupted cell-cell adhesion in

suspension, the effect of podocalyxin overexpression on cell-cell junctions in adherent cells

was next assessed.

Podocalyxin overexpression does not significantly alter cell junctions in

monolayer culture

While assessing the efficiency of mouse podocalyxin transgene expression, confluent

monolayers of OVCAR-3-podo and OVCAR-3-vector cells on glass coverslips were dual

stained for either E-cadherin/podocalyxin or ZO-1/podocalyxin (Fig. 6). Immunofluorescent

staining revealed no dramatic change in localization of the junctional proteins to points of

cell-cell contact. However, there appeared to be a subtle decrease in membranous E-cadherin localization in podocalyxin overexpressing cells, while ZO-1 localization was unchanged. Unfortunately, OVCAR-3-podo and OVCAR-3-vector cells exhibited a very flattened morphology when grown on glass coverslips as is evident from the confocal z sections. Since there was no distinction between apical and lateral membrane domains, I turned to assessing immunofluorescence of cell junctional proteins using cells grown on porous filter supports, which encouraged the cells to adopt a taller, cuboidal morphology.

Dual immunofluorescent staining was repeated using cells grown as confluent monolayers on filters with a 3 μm pore size (Fig. 8). Dual staining was performed for E-cadherin/podocalyxin and β-catenin/podocalyxin. Similarly to previous E-cadherin staining, immunofluorescent staining of OVCAR-3-podo monolayers on filters also showed a slight decrease in membranous E-cadherin. However, localization of β-catenin, another component of adherens junctions, did not appear to be altered by podocalyxin overexpression. This suggested that podocalyxin overexpression did not significantly disrupt adherens junctions in monolayers. To determine whether E-cadherin expression levels were altered by podocalyxin overexpression, Western blot analysis was performed on whole cell lysates. Similarly, cytoskeletal and soluble cell fractions were assessed for junctional protein levels to assess whether podocalyxin overexpression altered the subcellular localization of junctional protein in the cytoskeletal (ie junctional) or cytosolic compartment.

Figure 8. Podocalyxin overexpression does not significantly alter the localization of adherens junction proteins in OVCAR-3-podo monolayers.

Confluent monolayers of OVCAR-3-vector and OVCAR-3-podo cells were cultured on 3 μm pore filter inserts. Dual immunofluourescence staining was carried out using antibodies against A) mouse podocalyxin/E-cadherin, B) mouse podocalyxin/β-catenin. Confocal projections of xy slices with a corresponding z section are shown. (Scale bar = 10 μm).

A

OVCAR-3-vector | **OVCAR-3-podo**

E-cad/podo | E-cad | podo | E-cad/podo

B

OVCAR-3-vector | **OVCAR-3-podo**

β-catenin/podo | β-catenin | podo | β-catenin/podo
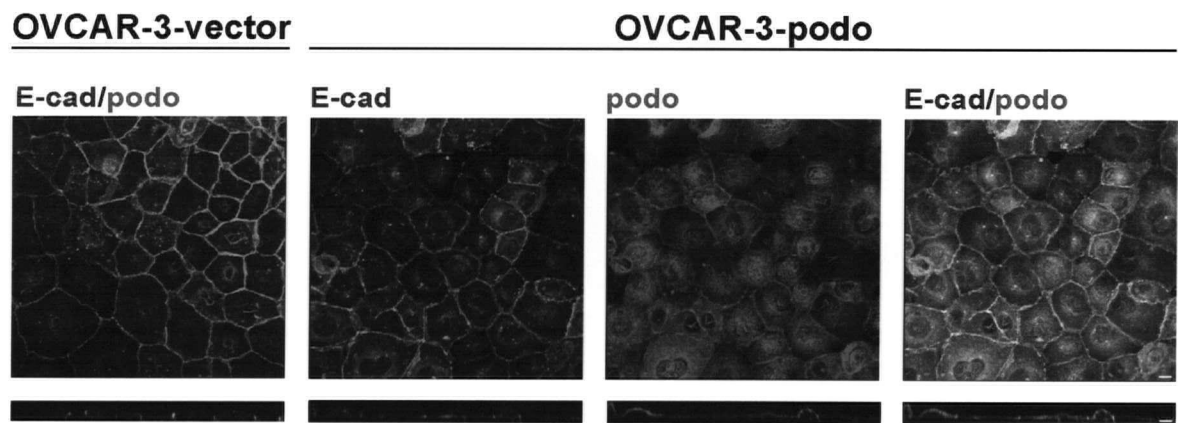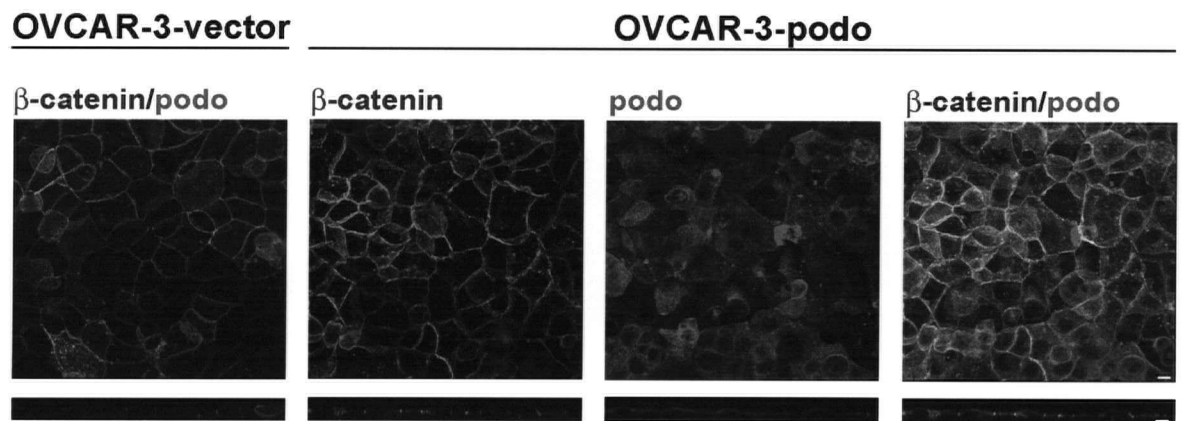
Western blot analysis for E-cadherin and mouse podocalyxin was performed using whole cell lysates prepared from parental OVCAR-3, OVCAR-3-vector, OVCAR-3-podo, parental OVCAR-8, OVCAR-8-vector, OVCAR-8-podo (Fig. 9). High levels of mouse podocalyxin were expressed by the FAC sorted OVCAR-3-podo population, whereas the OVCAR-8-podo cells expressed limited mouse podocalyxin, which is another reason the latter were not further characterized. There was no difference in E-cadherin expression levels between the parental cells, the vector control cells and the podocalyxin overexpressing cells. Since OVCAR-3-podo expressed mouse podocalyxin more efficiently than OVCAR-8-podo, the effects of podocalyxin overexpression on cell junction protein levels in soluble and cytoskeletal fractions were assessed using parental OVCAR-3, OVCAR-3-vector controls and OVCAR-3-podo. Western blot analysis for E-cadherin, β-catenin, α-catenin, p120 catenin, and ZO-1 was performed using the soluble and cytoskeletal fractions (Fig. 10). This evaluation of junctional proteins revealed that podocalyxin overexpression did not alter the proportion of junctional proteins that were localized to the cytoskeletal or cytosolic cell fractions. Therefore, podocalyxin overexpression did not alter the localization of junctional proteins in static, confluent monolayers. To assess whether podocalyxin overexpression may influence cell junction dynamics, localization of E-cadherin was next assessed during depolarization and repolarization of cell monolayers.

Podocalyxin overexpression in OVCAR-3 does not significantly alter adherens junction dynamics

The calcium switch assay is a manipulation that mimics the formation of a simple epithelial sheet (Adams et al., 1998; Adams et al., 1996; Yonemura et al., 1995). Calcium is

Figure 9. Ectopic overexpression of mouse podocalyxin in OVCAR-3-podo or OVCAR-8-podo cells is not associated with changes in E-cadherin expression.

Western blot analysis was performed on whole cell lysates derived from parental OVCAR-3, OVCAR-3-vector, OVCAR-3-podo, parental OVCAR-8, OVCAR-8-vector, OVCAR-8-podo. 40 μg of protein was resolved by SDS-PAGE and analyzed by Western blotting using antibodies against mouse podocalyxin and E-cadherin. 5 μg of lysate was probed for ERK1/2 to ensure equal protein concentration between samples. Parental OVCAR-3 and OVCAR-8 displayed verly low levels of endogenous podocalyxin (Figure 4), thus the bands present in all lanes of the mouse podocalxyin blot are likely due to non-specific antibody binding rather than cross-reactivity with human podocalyxin (arrows).

ERK 1/2 (42, 44 kDa)

E-cadherin (120 kDa)

ms podocalyxin (140 kDa)

OVCAR-3

OVCAR-3-vector

OVCAR-3-podo

OVCAR-8

OVCAR-8-vector

OVCAR-8-podo

36
50
98
149
50
64
98
149
250
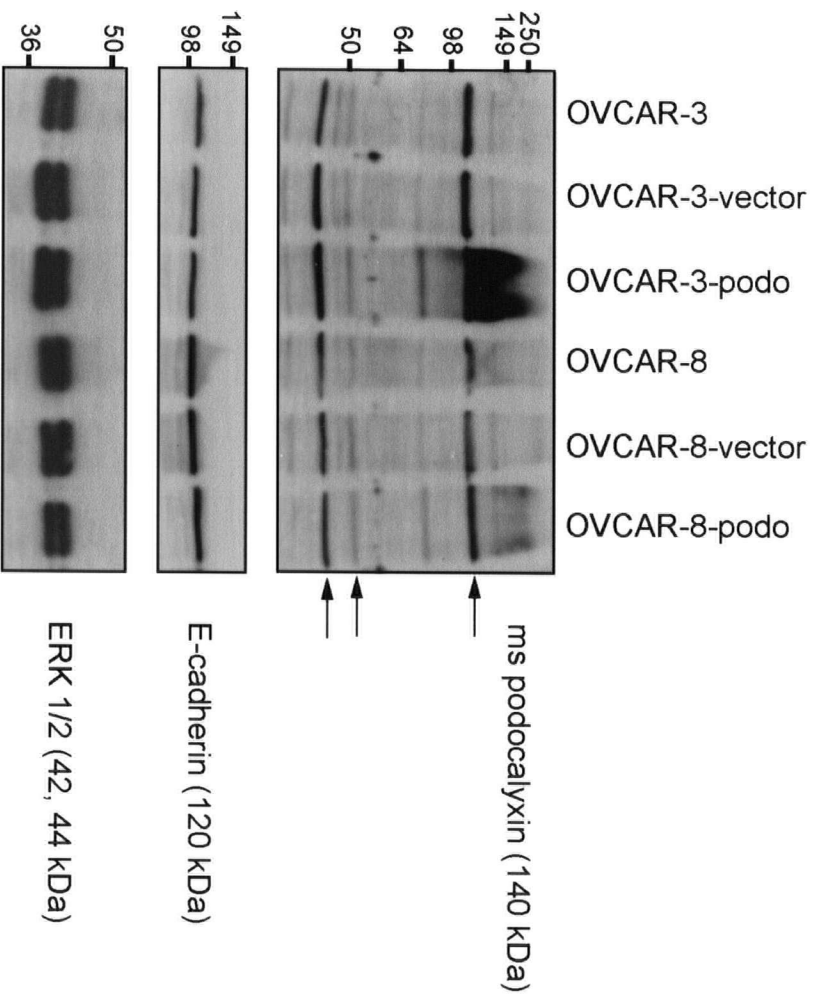
Figure 10. Podocalyxin overexpression does not alter the proportion of junctional protein in the cytoskeletal fraction.

Cell fractionation was performed by lysing parental OVCAR-3, OVCAR-3-vector and OVCAR-3-podo with 0.5% Triton-X 100 CSK buffer to isolate the soluble, cytosolic protein. The insoluble, cytoskeletal fraction was lysed by boiling and sonication with SDS-IP buffer. 40 μg of lysate was resolved by SDS-PAGE and analyzed by Western blotting using antibodies against mouse podocalyxin, E-cadherin, β-catenin, α-catenin, p120 catenin, and ZO-1. Since parental OVCAR-3 cells displayed verly low levels of endogenous podocalyxin (Figure 4), the smaller bands present in the mouse podocalxyin blot are likely due to non-specific antibody binding (arrows).

ms podocalyxin (140 kDa)

E-cadherin (120 kDa)

β-catenin (92 kDa)

α-catenin (102 kDa)

p120-catenin (120 kDa)

ZO-1 (225 kDa)
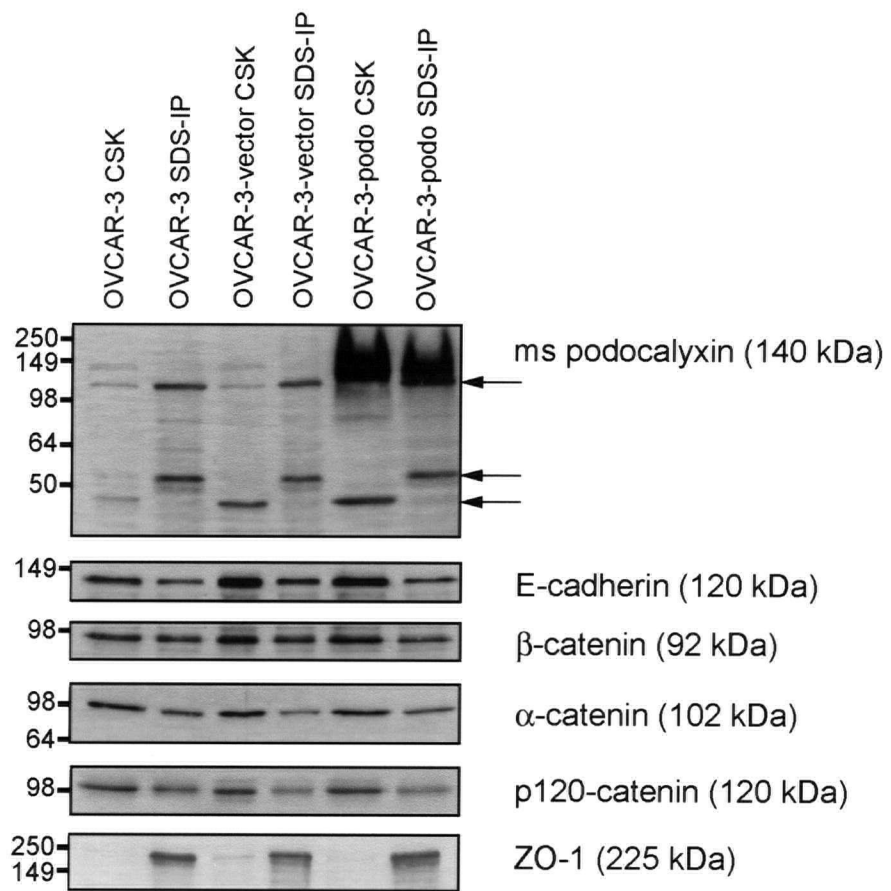
depleted from the culture media to prevent the calcium dependent conformational change in the E-cadherin extracellular domain that permits homophilic binding. Thus, when calcium is depleted from pre-formed cell monolayers, adherens junctions dissassemble and cells fail to form extensive cell-cell contacts. Despite attachment to the ECM, basolateral membrane proteins are randomly localized along the cell surface (Yeaman et al., 1999). Once calcium is increased, cells simultaneously re-assemble cell-cell junctional complexes. Therefore, a calcium switch can be applied to assess whether podocalyxin overexpression affects the rate of adherens junction dissassembly or re-assembly in monolayer culture.

Confluent monolayers on 3 μm filters were depleted of divalent cations by incubation with low calcium media (LCM) for three hours, and then switched to high calcium media (HCM) (Fig. 11). Before divalent cation depletion, ectopically expressed podocalyxin was localized to the apical membrane of OVCAR-3-podo cells and E-cadherin was localized to the basolateral membrane domain. Following calcium depletion, podocalyxin localization became more evenly distributed, yet remained excluded from the basal, substratum-attached membrane despite the dissassembly of adherens junctions. In low calcium conditions, vector control cells localized E-cadherin around the entire cell periphery. However, in podocalyxin overexpressing cells, E-cadherin was subtly depleted from the apical membrane domain of depolarized cells coinciding with regions where podocalyxin localized. The most obvious effect of podocalyxin overexpression on depolarized monolayers was greatly reduced cell adhesion to the substratum, which resulted in widespread delamination of the monolayer. Following addition of HCM, both vector control and podocalyxin overexpressing cells localized E-cadherin to points of cell-cell contact at a comparable rate, suggesting that

Figure 11. Podocalyxin overexpression does not perturb adherens junction dynamics.

A) Stable confluent monolayers of OVCAR-3-vector and OVCAR-3-podo cells on 3 μm

pore filters were subjected to depletion of divalent cations by incubating with low calcium

media (LCM), containing 5 uM $CaCl_2$, for three hours.

B) LCM was then replaced with high calcium media (HCM), 1.8 mM $CaCl_2$, to induce

simultaneous re-assembly of adherens junctions. Cells were fixed at the indicated time

points and dual immunostained for E-cadherin and mouse podocalyxin. Confocal projections

of xy sections with a corresponding z section are shown. (Scale bar = 10 μm).

A

	OVCAR-3-vector	OVCAR-3-podo		
	E-cad/podo	E-cad	podo	E-cad/podo

pre-LCM

30min LCM

60min LCM

3 hr LCM
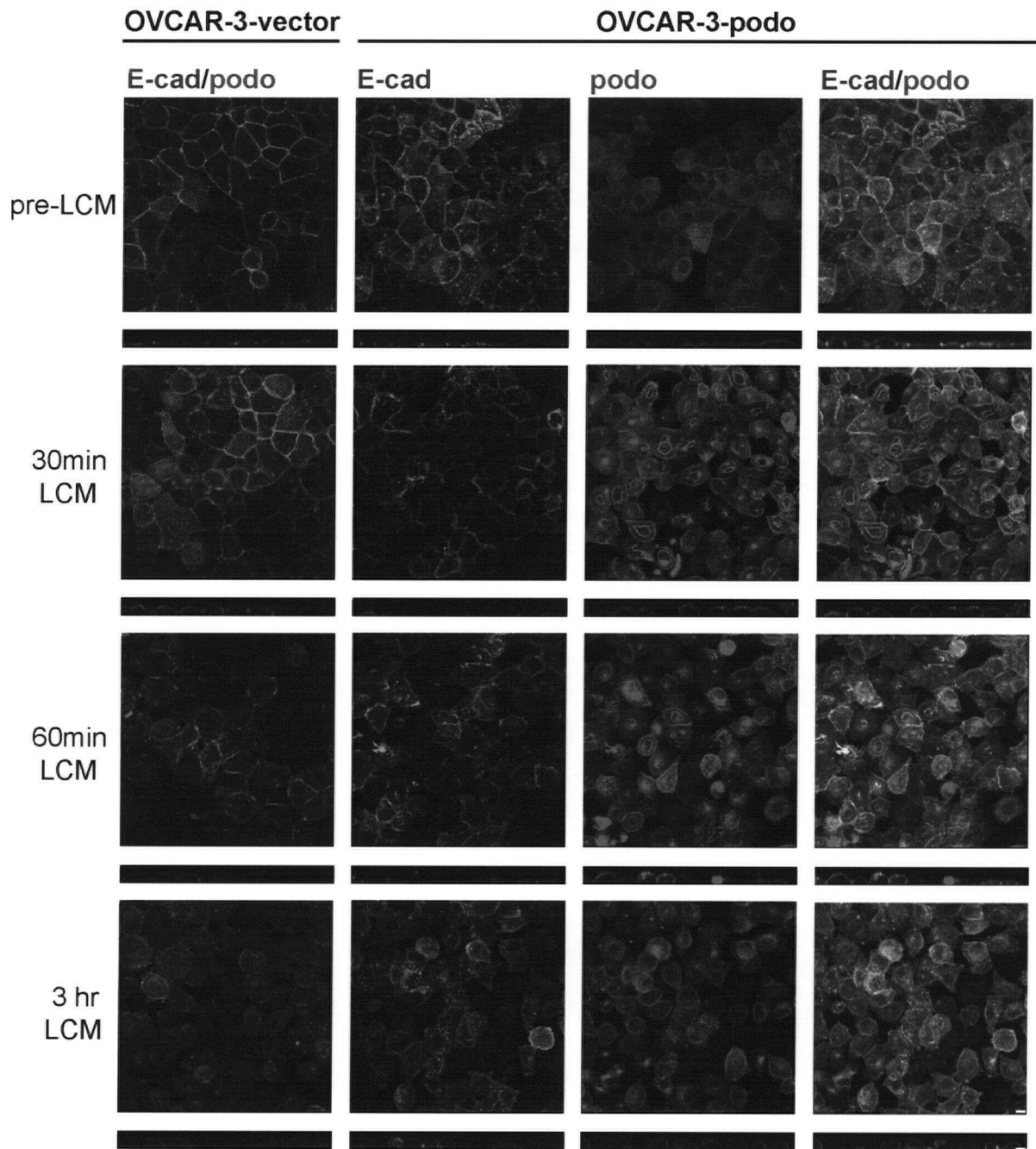
B
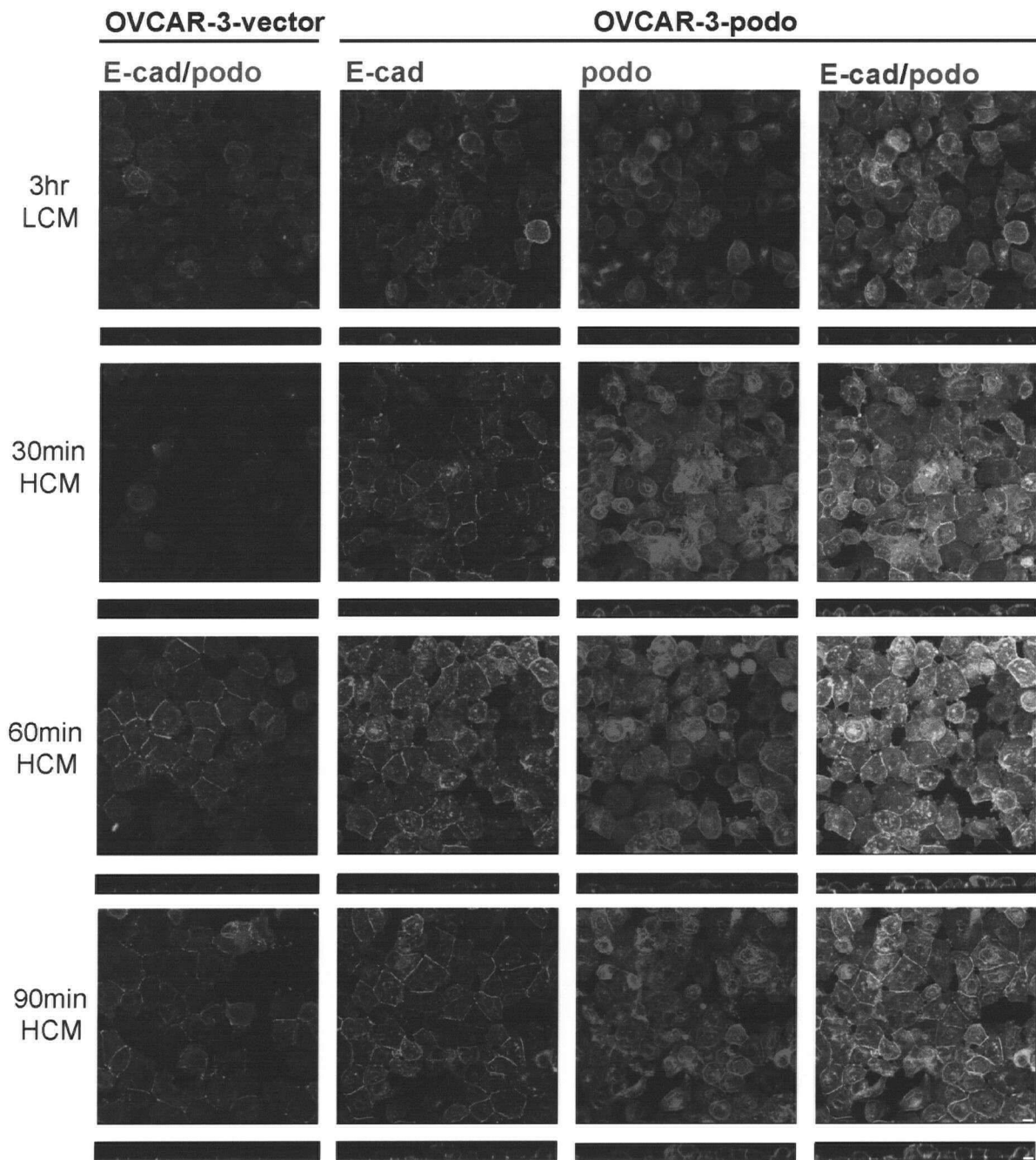
podocalyxin does not dramatically alter the dynamics of adherens junctions formation. In some fields of podocalyxin overexpressing cells, there appeared to be a delay in E-cadherin localization to cell-cell contacts but this was likely mainly due to defects in cell attachment to the substratum. Specifically, the podocalyxin overexpressing monolayers were less confluent following depolarization. Thus, the decrease in cell density was likely the cause of delayed adherens junction assembly after repolarization. Even OVCAR-3-podo cells that maintained adhesion to the substrata remained rounded up to one hour following addition of HCM, indicating a defect in cell spreading associated with the altered substratum adhesion. No clear disruption in adherens junction dynamics could be attributed to podocalyxin overexpression in confluent regions of the monolayer such as those shown in Fig. 11B. Altogether, these observations suggested that podocalyxin overexpression may disrupt cell-matrix adhesion.

Podocalyxin overexpression decreases cell-ECM adhesion

Fibronectin is an ECM with physiological relevance to ovarian carcinoma progression since fibronectin is synthesized by the peritoneal mesothelium (Cannistra et al., 1995). Thus, adhesion to the peritoneal wall, which enables attachment of ovarian carcinoma cells and invasion into the peritoneum, involves adhesion to a pericellular matrix rich in fibronectin (Cannistra et al., 1995) that is $\beta 1$ integrin-dependent (Lessan et al., 1999). Adhesion assays to fibronectin-coated wells revealed that podocalyxin overexpression dramatically reduced adhesion (Fig. 12A). Adhesion of OVCAR-3-podo cells to fibronectin was inhibited by over 50% compared to vector control cells (Fig. 12A). To more closely model adhesion of ovarian carcinoma cells to the mesothelial lining of the peritoneal wall, adhesion assays were

Figure 12. Podocalyxin overexpression decreases cell adhesion to fibronectin and to mesothelial cell monolayers.

Cell adhesion of OVCAR-3-vector and OVCAR-3-podo cell suspensions to either:

A) bovine serum fibronectin-coated wells (25 μg/ml) or B) live HUITLP9 mesothelial cell monolayers was assessed. The data are expressed as percent adhesion by dividing fluorescence of adherent cells/total fluorescence (mean +/- SD, n=3). To assess the contribution of non-specific adhesion, cell adhesion to 1% bovine serum albumin (BSA) was assessed as a negative control.

A
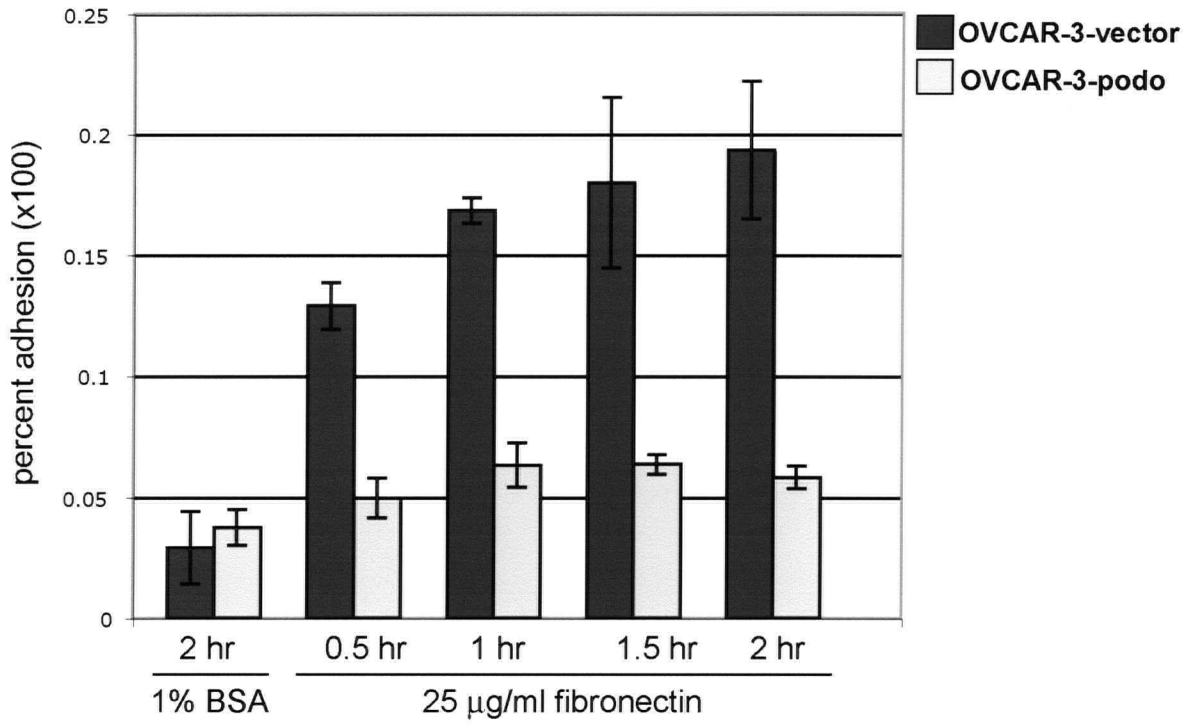
B
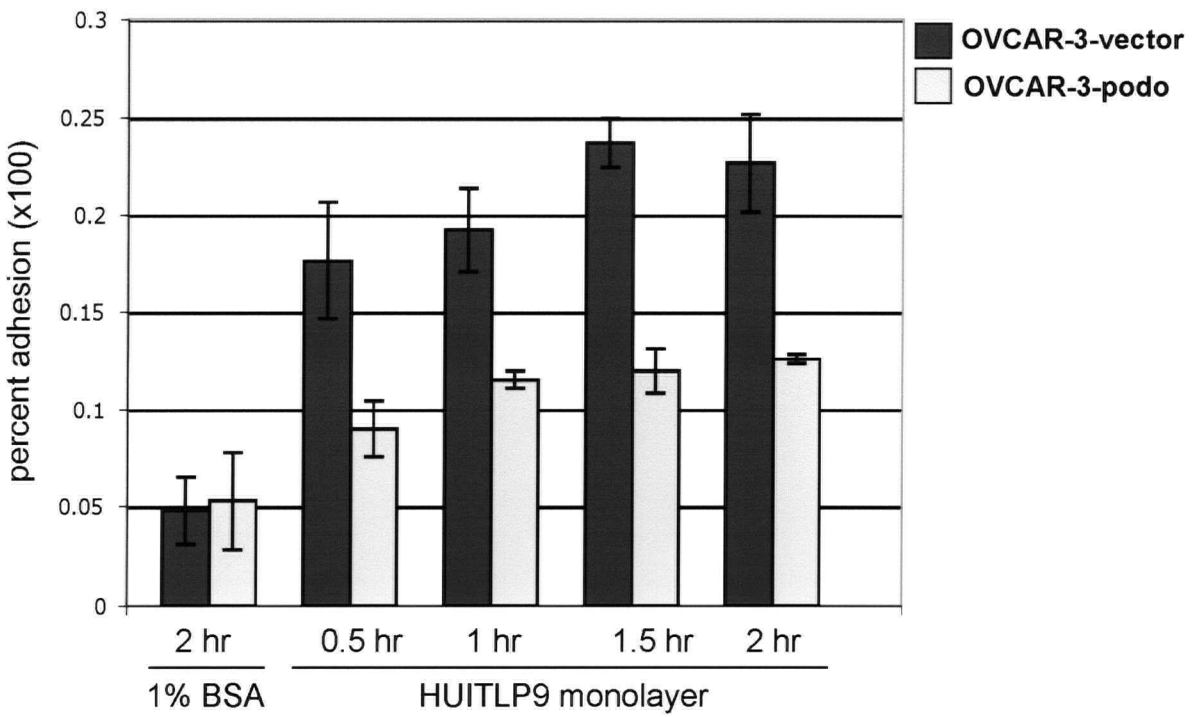
performed using a confluent monolayer of immortalized human mesothelial cells, HUITLP9, as an adhesive substrate for cell attachment. Adhesion of OVCAR-3- podo cells to HUITLP9 monolayers was inhibited by nearly 50% compared to vector control cells throughout the time course (Fig. 12B). Therefore, podocalyxin overexpression dramatically disrupts cell-matrix adhesion of OVCAR-3 cells.

As I observed for cell-cell aggregation, podocalyxin's anti-adhesive properties are, at least in part, conferred by its bulky and highly negatively charged ectodomain. To determine whether both of these properties, negative charge and steric hindrance, or negative charge alone reduce cell-ECM adhesion, enzymatic treatments were performed to alter the podocalyxin ectodomain prior to adhesion asssays to fibronectin (Fig. 13A). O-sialoglycoprotein endopeptidase removes the bulky and negatively charged mucin domain from podocalyxin's ectodomain. Neuraminidase (sialidase) cleaves sialic acid residues and can be used as a tool to assess the contribution of negatively charged sialic acid residues to podocalxyin's anti-adhesive effects (Takeda et al., 2000). As previously mentioned for endopeptidase, these enzymatic treatments are not specific to podocalyxin and will also alter the structure of other glycoproteins at the cell surface. OVCAR-3-podo and OVCAR-3-vector cells were either untreated or pre-treated with sialidase or endopeptidase. Cells were then plated on fibronectin-coated wells and the percentage of cells attached after 90 min was quantified. To verify the enzymatic treatments were successful, cells were treated separately alongside those fluorescently labelled for the adhesion assay and lysed for Western blot analysis of ectopic mouse podocalyxin (Fig. 13B). As expected, no podocalyxin was observed in the OVCAR-vector cells. A band corresponding to the molecular weight of full-

Figure 13. Podocalyxin's anti-adhesive properties can be partially reversed by enzymatic digestion of the podocalyxin ectodomain.

A) Cell adhesion to 25 µg/ml bovine serum fibronectin-coated wells was assessed following a 90 min incubation of untreated, 250 mU/ml neuraminidase (sialidase) treated or 0.2 µg/µl O-sialoglycoprotein endopeptidase treated OVCAR-3-vector and OVCAR-3-podo single cell suspensions. To assess the contribution of non-specific adhesion, cell adhesion of untreated cells to 1% bovine serum albumin (BSA) was assessed as a negative control. The data are expressed as percent adhesion by dividing fluorescence of adherent cells/total fluorescence (mean +/- SD, n=3).

B) Western blot analysis for mouse podocalyxin in untreated, sialidase treated and endopeptidase treated OVCAR-3-vector and OVCAR-3-podo cells.

C) Following removal of unattached cells in A), adherent untreated, neuraminidase treated or endopeptidase treated cells were imaged by phase-contrast microscopy.

A

B

C

length podocalxyin was observed in the OVCAR-3-podo untreated cells. A higher molecular weight band was observed in the sialidase treated OVCAR-3-podo cells, consistent with succesful enzymatic digestion of sialic acid residues (Takeda et al., 2000). For the O-sialoglycoprotein endopeptidase treated OVCAR-3-podo cells, a faint band was detected, suggesting partial cleavage of podocalyxin ectodomain. The absence of a band would have been consistent with complete cleavage of mucin domain cleavage, since this is the domain against which the anti-mouse podocalyxin antibody was raised. Western blot analysis of mouse podocalyxin in cells subjected to enzymatic digestion revealed alterations in the molecular weight of mouse podocalyxin that were consistent with efficient enzymatic treatments.

Neuraminidase treatment to remove sialic acid residues from the ectodomain of sialylated glycoproteins such as podocalyxin caused a slight increase in adhesion to fibronectin in both OVCAR-3-vector and OVCAR-3-podo cells. Neuraminidase treatment of OVCAR-3-vector caused a slight increase in cell adhesion compared to untreated cells due to non-specific cleavage of sialic acid residues from sialoproteins other than podocalyxin. Neuraminidase treatment of OVCAR-3-podo cells also resulted in a small increase in cell adhesion compared to untreated cells. Neuraminidase treatment caused a greater relative increase in cell adhesion in OVCAR-3-podo cells suggesting that sialic acid residues in the podocalyxin ectodomain play a minor role in anti-adhesion. Endopeptidase treatment to remove the bulk and negative charge of podocalyxin's ectodomain reverted the anti-adhesion of OVCAR-3-podo cells 2.3-fold compared to untreated OVCAR-3-podo. However, endopeptidase treatment of the vector control cells resulted in a 1.5-fold increase in adhesion,

likely resulting from mucin domain cleavage of other glycoproteins. Although not as striking as the endopeptidase-induced reversal of cell-cell aggregation, endopeptidase treated OVCAR-3-podo cells displayed a higher fold increase in cell-ECM adhesion than endopeptidase treated OVCAR-3-vector cells. In conclusion, removal of the bulk and negative charge of podocalyxin's extracellular domain contributes partly to reversal of the anti-adhesive phenotype.

$\beta1$ integrin engagement is disrupted by podocalyxin overexpression

Podocalyxin overexpression dramatically decreased adhesion to fibronectin, in part via its bulky, negatively charged ectodomain. Since adhesion of ovarian carcinoma cells to the peritoneal mesothelial LP9 cells depends partly on $\beta1$ integrin function (Lessan et al., 1999) and β_1-integrin is one of the integrin subunits that acts as a receptor for fibronectin, I reasoned that podocalyxin may decrease cell adhesion by interfering with $\beta1$ integrin engagement. To assess this, cell adhesion assays were performed using an immobilized anti-$\beta1$ integrin antibody as a substrate (Fig. 14A). The P5D2 mouse monocloncal $\beta1$ integrin antibody recognizes the extracellular domain of $\beta1$ integrins (Seltzer et al., 1994; Takada and Puzon, 1993). Podocalyxin overexpressing cells exhibited a 66% decrease in adhesion to 20 ug/ml of P5D2 antibody relative to vector control cells. Since podocalyxin overexpression does not alter the levels of $\beta1$ integrin protein (Fig. 14C), it is likely that podocalyxin disrupts adhesion by interfering with integrin engagement.

Figure 14. Podocalyxin overexpression decreases engagement of the β1 integrin extracellular domain.

A) Cell adhesion assays were performed using 10 µg/ml or 20 µg/ml immobilized anti-β1 integrin P5D2 antibody as a substrate. To assess the contribution of non-specific adhesion, cell adhesion to 1% bovine serum albumin (BSA) was assessed as a negative control. The data are expressed as percent adhesion by dividing fluorescence of adherent cells/total fluorescence (mean +/- SD, n=3).

B) Following removal of unattached cells, cells adhering to 20 ug/ml β1 integrin antibody in A) were imaged by phase-contrast microscopy.

C) Western blot analysis of β1 integrin expression in 40 µg of whole cell lysate isolated from parental OVCAR-3, OVCAR-3-vector, OVCAR-3-podo.

A

percent adhesion (x100)

- OVCAR-3-vector
- OVCAR-3-podo

1% BSA

β1 integrin antibody
10 μg/ml   20 μg/ml

B

	1% BSA	β1 integrin antibody
OVCAR-3-vector		
OVCAR-3-podo		

C

148 —
98 —

β1 integrin (130 kDa)

50 —
36 —

ERK 1/2 (42, 44 kDa)

OVCAR-3   OVCAR-3-vector   OVCAR-3-podo
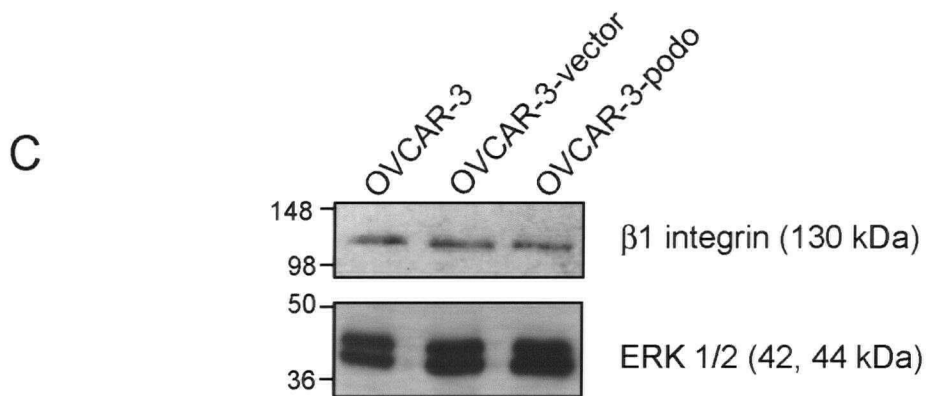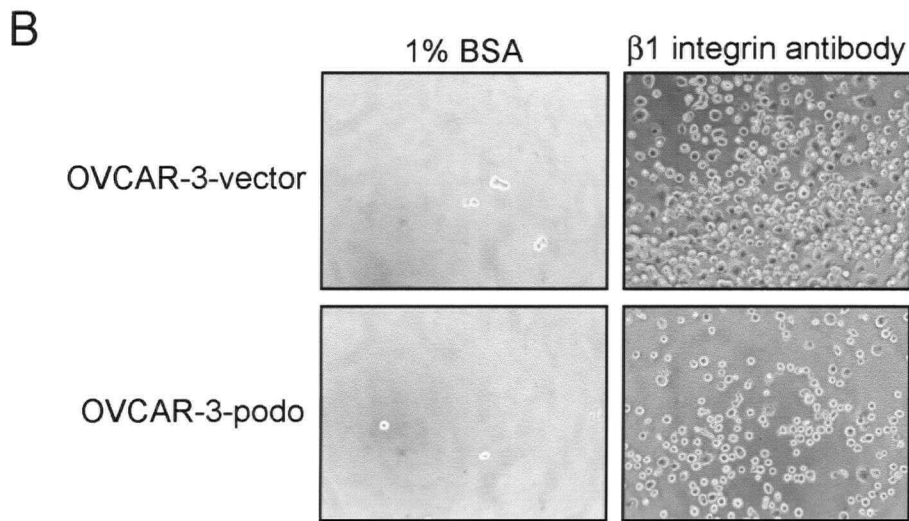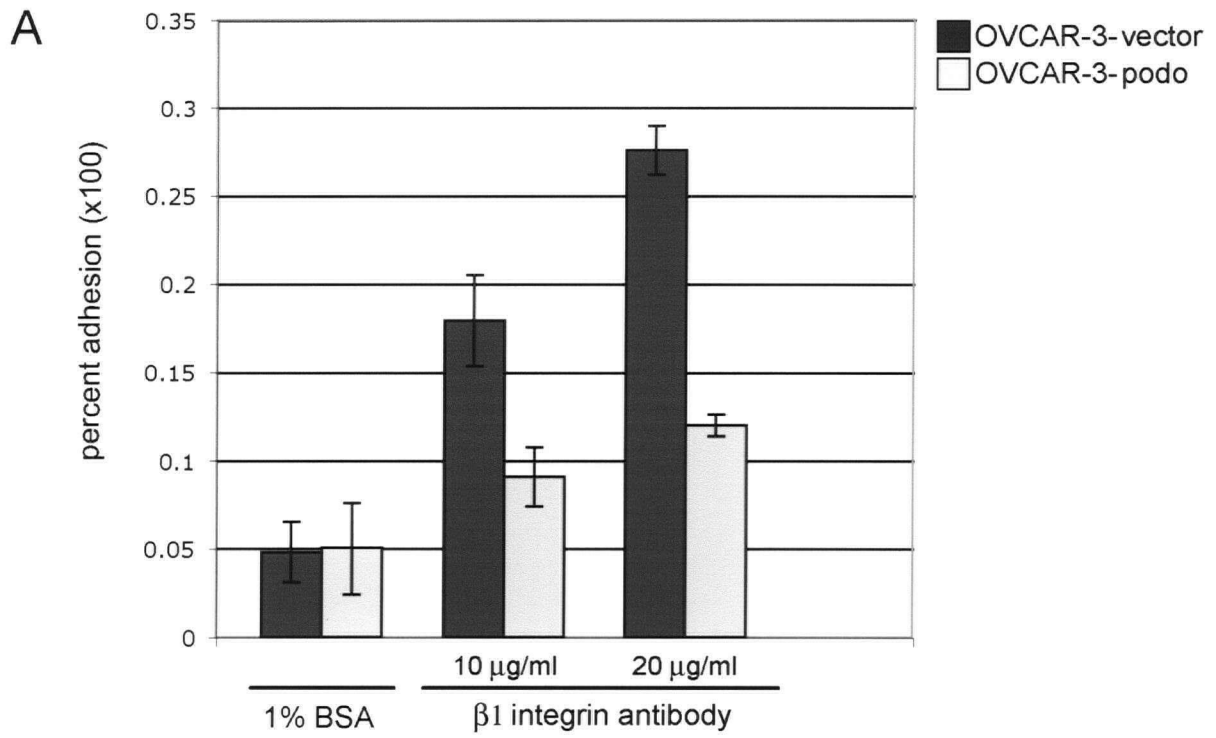
β1 integrin segregates from podocalyxin during cell attachment

Although adhesion was dramatically reduced, a small percentage of single, suspended OVCAR-3-podo cells were nonetheless able to attach to fibronectin, HUITLP9 cells or anti-β1 integrin antibody-coated wells (Fig. 13, 14). Therefore, the anti-adhesive effects of podocalyxin were not absolute and were overcome in certain cells to enable integrin engagement and cell attachment. To analyze podocalyxin and β1 integrin localization in single cells in the early stages of attachment, dual immunofluorescence staining was performed (Fig. 15). In these single cell attachment assays, podocalyxin localized assymetrically in the membrane such that it localized to the free surface of the cell and was excluded from the basal surface of the cell wherever it contacted the substratum. Dual immunofluorescent staining revealed that β1 integrin and podocalyxin localization could overlap except at sites of membrane ruffling where cell-ECM adhesion is highly dynamic.

Podocalyxin restricts the apical localization of β1 integrin in 2D monolayers

Confluent monolayers of podocalyxin overexpressing cells on porous filters have consistently localized podocalyxin to the apical domain. To assess how podocalyxin overexpression effects β1 integrin localization in these fully polarized monolayers, dual immunofluorescence staining for podocalyxin and β1 integrin was carried out (Fig. 16). In OVCAR-3-vector cells, β1 integrin was distributed evenly to the cell periphery. As expected, in OVCAR-3-podo cells, podocalyxin localized exclusively to the apical domain. High levels of podocalyxin localization resulted in expansion of the apical domain, which gave the cells a rounded, bulging phenotype. β1 integrin localized predominantly to the basolateral membrane domain in the latter cells and its staining was depleted from the free

Figure 15. Podocalyxin and β1 integrin are partly segregated during early stages of single cell attachment.

Four hours after plating sparse, single cell suspensions of OVCAR-3-vector and OVCAR-3-podo cells onto glass coverslips, cells were fixed and dual immunofluorescently stained for podocalyxin/β1 integrin. Confocal xy projections and a corresponding z sections are shown. (Scale bar = 10 μm).

OVCAR-3-vector

OVCAR-3-podo

β1 integrin/podo   β1 integrin   podo   β1 integrin/podo
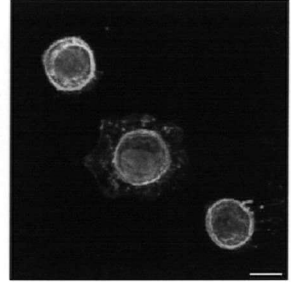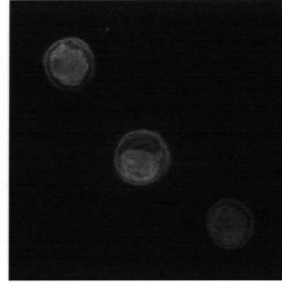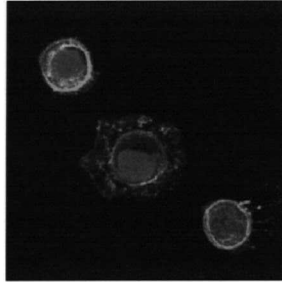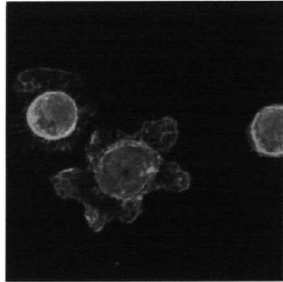
Figure 16. Podocalyxin overexpression alters the localization of β1 integrin in static monolayers of OVCAR-3-podo cells.

Dual immunofluorescent staining for β1 integrin/podocalyxin was performed on confluent monolayers of OVCAR-3-vector and OVCAR-3-podo cells on 3 μm pore filters. Podocalyxin localization to the apical domain (arrowheads) was associated with depleted β1 integrin localization. Confocal projections of xy sections as well as a corresponding z section are shown (Scale bars = 10 μm).

OVCAR-3-vector

OVCAR-3-podo

β1 integrin/podo   β1 integrin   podo   β1 integrin/podo
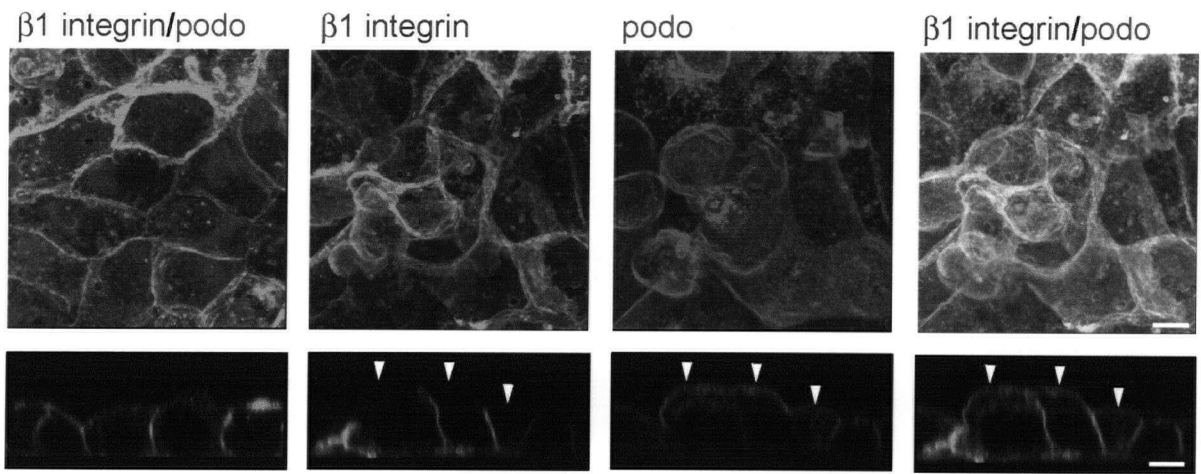
apical surface, precisely where podocalyxin was targetted. Thus, localization of podocalyxin to the apical membrane in confluent monolayers results in depletion of β1 integrin from these sites.

A calcium switch was next employed to assess whether podocalyxin overexpression influences integrin localization during depolarization or repolarization (Fig. 17). As a confluent monolayer on a porous filter substratum, OVCAR-3-vector cells displayed evenly distributed β1 integrin at the cell periphery. Podocalyxin overexpressing monolayers targetted podocalyxin exclusively to their apical domain and this was associated with a subtle depletion of β1 integrin from this site both before low calcium medium treatment (LCM) and following LCM treatment when adherens junctions were dissassembled (Fig. 17A). Upon readdition of high calcium medium (HCM), adherens junctions re-assembled and β1 integrin localized to cell contacts at similar rates in both OVCAR-3-vector and OVCAR-3-podo cells (Fig 17B). As was evident previously in calcium switch experiments, podocalyxin overexpression delayed cell spreading upon repolarization, perhaps because integrin localization was restricted by podocalyxin.

Podocalyxin restricts the localization of β1 integrin in 3D clusters

To investigate the consequences of podocalyxin overexpression on cell-matrix interactions in a three-dimensional context, cell clusters were cultured in reconsituted basement membrane (Matrigel) and then assessed for podocalyxin and β1 integrin localization (Fig. 18). OVCAR-3 cells did not fully polarize in this context, although they were able to form cell clusters. In contrast, 3D cultures of OVCAR-8 cells yielded some

Figure 17. Podocalyxin overexpression alters the localization of β1 integrin in depolarized monolayers and delays cell spreading upon repolarization.

A) Stable confluent cell monolayers on 3 μm pore filters were subjected to depletion of divalent cations by incubation with low calcium media (LCM) (5 uM CaCl2) for three hours. B) Following divalent cation depletion, media was switched to high calcium media (HCM) (1.8 mM CaCl2) to re-assemble adherens junctions. Cells were fixed and dual immunostained for β1 integrin/podocalyxin at the indicated time points. Confocal projections of xy sections as well as a corresponding z section are shown (Scale bars = 10 μm).

A

OVCAR-3-vector | OVCAR-3-podo

β1 integrin/podo | β1 integrin | podo | β1 integrin/podo

pre-LCM

30 min LCM

60 min LCM

3 hr LCM

84

B

OVCAR-3-vector   OVCAR-3-podo

β1 integrin/podo   β1 integrin   podo   β1 integrin/podo

3 hr LCM

30 min HCM

60 min HCM

120 min HCM
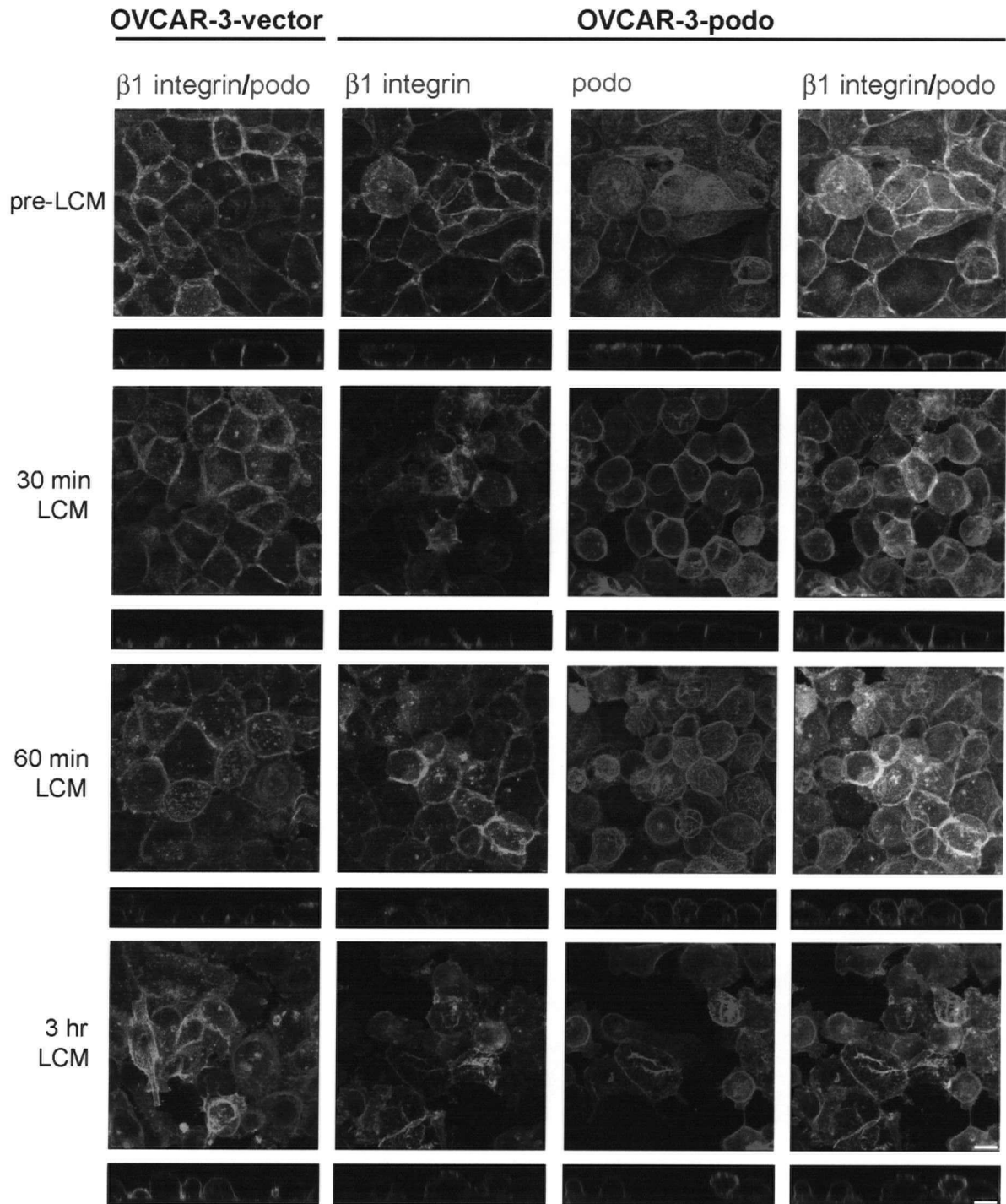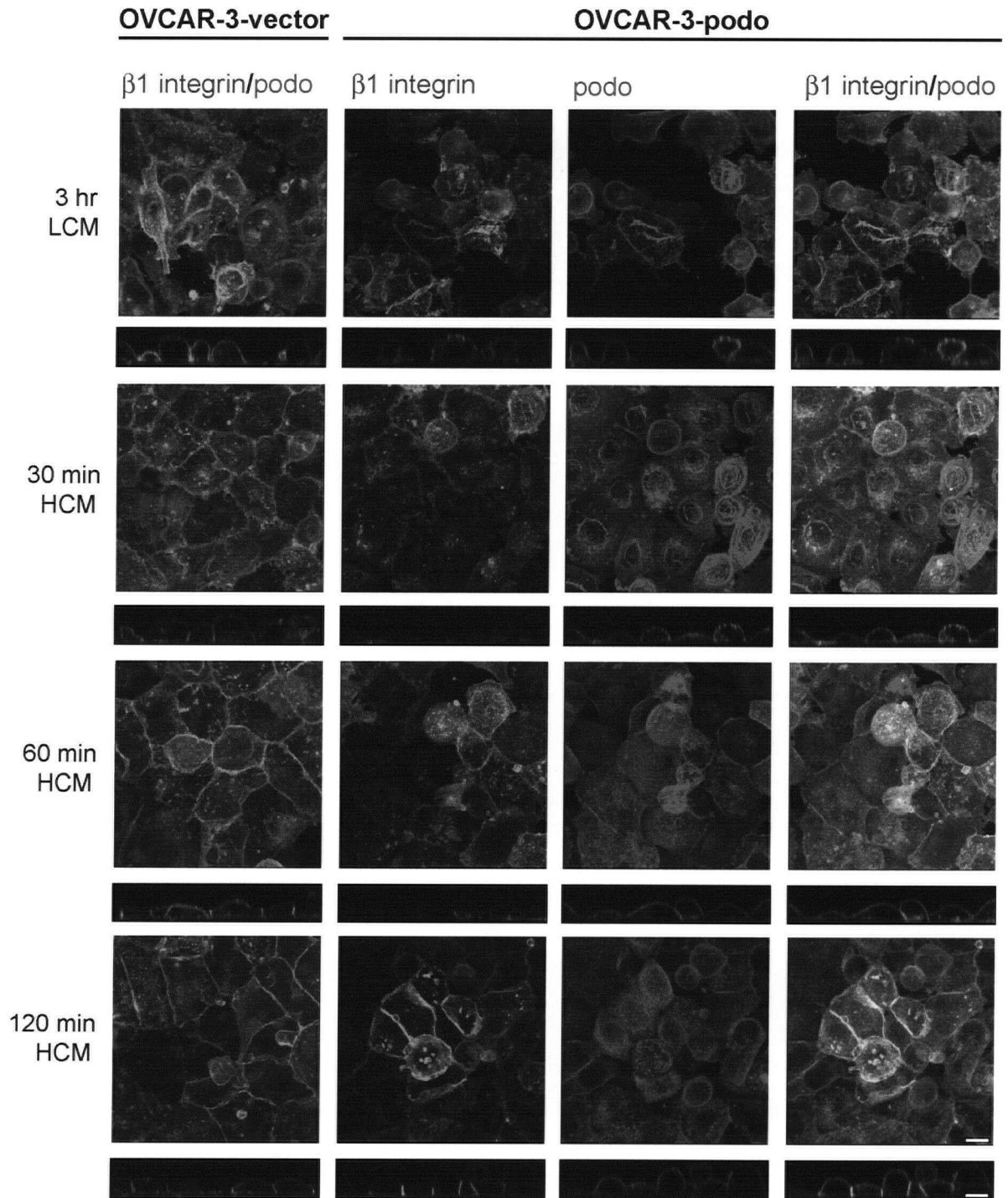
polarized spheroids and thus OVCAR-8-podo cells were also assessed for podocalyxin/β1

integrin localization under these conditions. Full polarization in the latter spheroids was

characterized by localization of apical membrane proteins towards the centre of the spheroid

and basal proteins to the outside surface of the spheroid. When OVCAR-3-vector cells were

cultured in Matrigel, β1 integrin was evenly distributed to the cell periphery at points of cell-

matrix and cell-cell contact. However, in OVCAR-3-podo cell clusters, podocalyxin was

localized to the cell-matrix interface of 3D cell clusters (Fig. 18A) presumably due to the

polarity disruption. Regardless, β1 integrin was depleted from the membrane domain where

podocalyxin was targetted (arrowheads), while β1 integrin localization at cell-cell contacts

was unaffected. Additionally, OVCAR-3-podo cells in the centre of the 3D clusters with no

free surface did not target podocalyxin to points of cell-cell contact and protein remained

localized inside the cell. This suggests that in the absence of a free surface, podocalyxin may

not be targetted to the membrane.

In contrast to OVCAR-8-podo monolayers (Fig. 6), 3D cultures of OVCAR-8-podo

cells exhibited efficient targetting of ectopic podocalyxin to the membrane (Fig. 18B). In 3D

cultures, a fraction of OVCAR-8-podo cells were capable of polarized spheroid formation on

Matrigel as is evident by the localization of podocalyxin, an apical marker, towards a central

lumen. In these polarized OVCAR-8-podo cells β1 integrin localized to the basolateral

surface of the cluster and was excluded from the apical membrane domain where

podocalyxin was targetted (arrowheads). In contrast, non-polar OVCAR-8-podo cells

localized podocalyxin to the cell-matrix interface of the spheroid, and as was the case with

OVCAR-3-podo spheroids, β1 integrin was excluded (Fig.18A) (arrowheads). In conclusion,

Figure 18. Podocalyxin localization to the cell-matrix interface restricts β1 integrin accumulation.

Spheroids were generated by culturing cells as clusters on Matrigel for five days. Spheroids were fixed and dual immunostained for β1 integrin/podocalxyin.

A) OVCAR-3-vector and OVCAR-3-podo cells were not capable of polarized spheroid formation on matrigel since podocalyxin, an apical marker, did not localize towards a central lumen. Podocalyxin localized to the cell-matrix interface of non-polar clusters, and restricted the localization of β1 integrin to this domain (arrowheads) compared with cells not expressing podocalyxin.

B) OVCAR-8-podo cells were capable of polarized spheroid formation on matrigel since podocalyxin, an apical marker, localized to the central lumen (arrows). In non-polar OVCAR-8-podo spheroids localization of podocalyxin to the cell-matrix interface of the spheroid was associated with exclusion of β1 integrin (arrows). Images are confocal xy slices taken through the centre of the cluster. (Scale bar = 10 μm).

A

OVCAR-3-vector　　　　　　　　**OVCAR-3-podo**

β1 integrin/podo　　β1 integrin　　　podo　　　β1 integrin/podo

B

OVCAR-8-vector　　　　　　　　**OVCAR-8-podo**
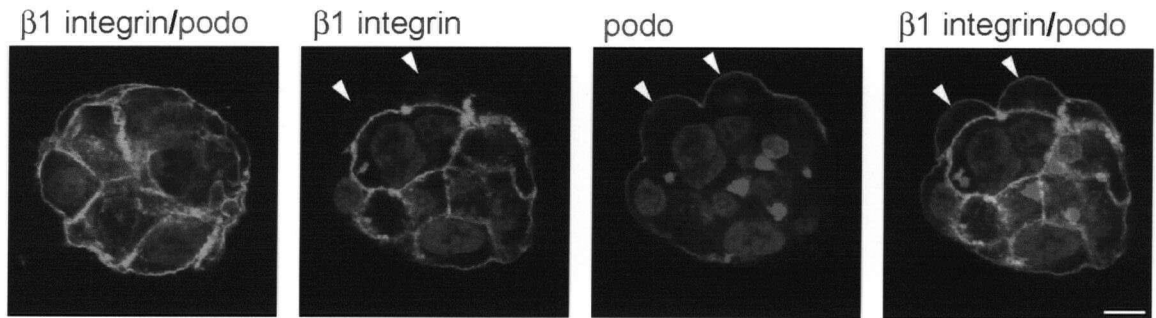
β1 integrin/podo　　β1 integrin　　　podo　　　β1 integrin/podo
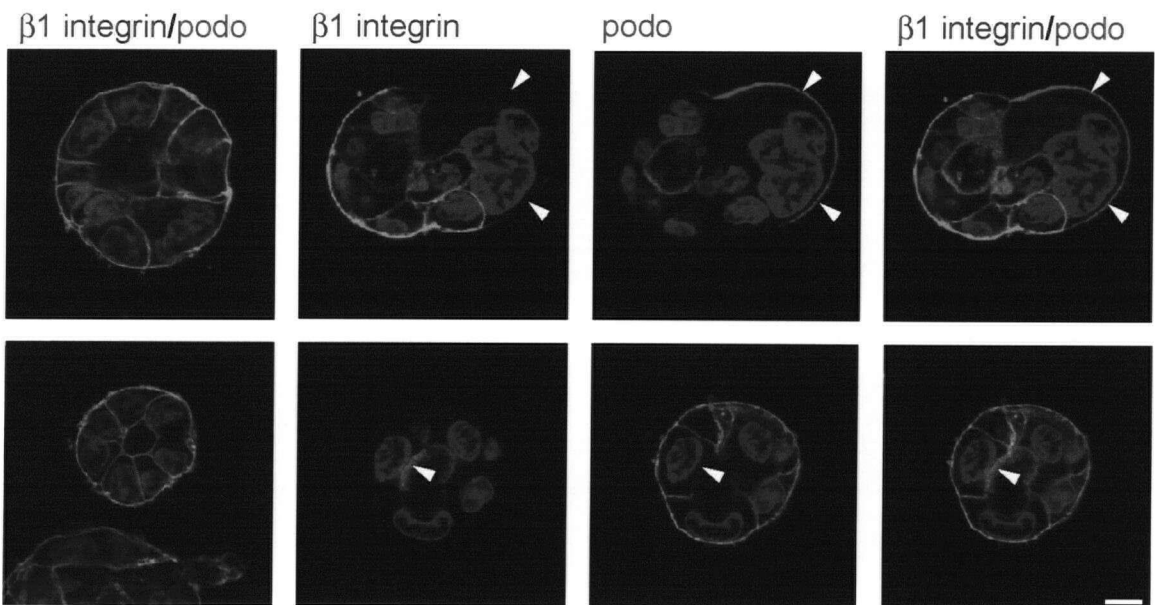
when podocalyxin localizes asymmetrically, as seen in 2D monolayers or polarized 3D spheroids, it restricts localization of the β1 integrin subunit. As a result, when polarity is disrupted the redistribution of podocalyxin may exclude β1 integrins and thereby disrupt cell-ECM interactions.

4. DISCUSSION

Unlike carcinomas that arise in other other epithelial tissues, ovarian carcinoma formation involves the emergence of a highly-differentiated intermediate which is associated with the induction of E-cadherin expression (Auersperg et al., 2001). Another distinctive feature of ovarian carcinoma progression is the route of dissemination of the primary neoplasm which, instead of relying on intravasation into the vasculature as the primary metastatic route, often involves direct release of tumour cells from the surface of the ovary into the peritoneal cavity. A significant proportion of these ovarian carcinoma cells suspended in patient ascites have been shown to exist as single cells or loose multi-cellular tumour aggregates, a portion of which become loosely attached to the extraovarian mesothelial wall (Allen et al., 1987). Based on the prevalence of such attached nodules at the time of surgery in patients with ascites, it is presumed that a very small proportion of them become invasive and locally metastatic as the disease progresses (Burleson et al., 2004). Regardless of the precise sequence and timing of these events, which are not precisely known, and given the absence of reliable animal models of the disease, it is clear that ovarian carcinoma cells must dynamically alter their adhesive properties to transition between the different environments encountered along this metastatic route. Thus, the identification of modifiers of cell adhesion in ovarian cancer is an important research goal. Podocalyxin may be one such adhesion modifier.

I found that podocalyxin is expressed by the OSE, which is thought to be the cell type of origin of ovarian carcinomas. Podocalyxin is also expressed in Mullerian duct-derived

female reproductive tract epithelia, which may also undergo malignant transformation in some circumstances. It is also expressed, often at very high levels, in the majority of ovarian carcinomas, particularly in tumours of the most prevalent serous subtype. My preliminary functional assays indicate that podocalyxin overexpression decreases ovarian carcinoma cell-cell aggregation and cellular interactions with the ECM. These data are consistent with the notion that podocalyxin could potentially play a functional role in the shedding of ovarian tumor cells into the peritoneal cavity during the initial steps of metastasis. Interestingly, my immunohistochemical observations also suggest that the podocalyxin molecule itself may be shed from the surface of ovarian tumor cells. Thus, it may be a potential serum and/or ascitic marker of the disease.

The *in vitro* assays used here illustrate how changes in cell polarity may modulate the phenotypic effects of podocalyxin overexpression. In polarized monolayers, ectopic, force-expressed podocalyxin was apically targetted and it caused an apical bulging of the plasma membrane. Ectopic podocalxyin also restricted the localization of β1 integrin in theses monolayers by depleting them from the apical membrane domain. Importantly, however, ectopic podocalyxin itself did not disrupt cell polarity or cell-cell junctions in stable cell monolayers as the subcelluar localization of E-cadherin and ZO-1 was not affected. In contast, ectopic podocalyxin inhibited the aggregation of single cells in suspension in a mucin domain-dependent manner. Similarly, the adhesion of single suspended cells to fibronectin was dramatically decreased, likely because podocalyxin's mucin domain interfered with integrin engagement to the matrix. Thus, podocalyxin's localization along the entire cell surface may enable its extracellular mucin domain to mask cell-cell adhesion

molecules and integrins in single, suspended cells. Importantly, ectopic podocalyxin expression also decreased the adhesion of ovarian carcinoma cells to mesothelial cells *in vitro*. Thus, podocalyxin expression may be downregulated in secondary extraovarian peritoneal lesions, a possibility that has not yet been investigated.

Although podocalyxin overexpression did not disrupt polarity in stable monolayers, it may influence cell polarity during ovarian carcinoma progression. Podocalyxin, which is the human homologue of canine gp135, has recently been identified as a necessary component for polarization of canine kidney MDCK cell cysts in 3-D collagen gel (Meder et al., 2005). Like single, attached podocalyxin overexpressing OVCAR-3 cells, single MDCK cells also exhibited assymetric localization of gp135 such that its localization was excluded from the basal, attached surface. gp135, along with one of its binding partners NHERF-2, were proposed to be involved in the formation of a pre-apical membrane scaffold in MDCK cells that may recruit polarity proteins (Meder et al., 2005). These authors proposed that gp135 exhibited polarized apical targetting in the absence of adherens junctions. It is also possible that podocalyxin is excluded from basal membrane contacts due to the biophysical properties of its bulky extracellular domain, which may also be the reason for podocalyxin redistribution to non-adhesive membrane domains in other cellular contexts (Tan et al., 2006). Since integrins, like most other cell surface molecules, do not extend upwards of 30 nm from the cell membrane (Becker et al., 1989; Hynes, 1992) during integrin engagement the basal membrane would undergo a close apposition to the substrata. Thus, once they are engaged with the matrix, integrins may exclude podocalyxin from the basal membrane domain since the latter molecule's extracellular domain likely extends beyond the space due

to its bulky glycosylation. Such an exclusion of podocalyxin from the attached basal domain was clearly evident during single cell attachment assays. Specifically, podocalyxin was absent from membrane ruffles where β1 integrin was highly concentrated. Additionally, since podocalyxin was not targetted to the membrane by spheroid cells lacking a free surface, this also suggests that podocalyxin's extracellular domain may prevent its incorporation into adhesive membrane domains. Whether by virtue of its biophysical properties described above, or due to differential membrane domain trafficking, podocalyxin was assymetrically localized in single, attached cells in the absence of cell-cell junctions. Therefore, by creating membrane assymmetry, podocalyxin may mark the identity of the apical membrane domain during the earliest stages of cell polarization and participate in the formation of a scaffold rich in PDZ-domain containing proteins for the recruitment of polarity proteins.

Although polarity proteins are required for cell polarization, their activity and expression are tightly regulated to prevent imbalances that disrupt apical-basal polarity. aPKC, the sole catalytic subunit of the Par3/Par6/aPKC complex, is required for the establishment and maintenance of cell polarity, adherens junctions and tight junctions (Macara et al., 2004). However, overexpression of the activated form disrupts apical-basal polarity in serous epithelial ovarian cancers (Eder et al., 2005). Similarly, even though it may be required for polarization, overexpression of podocalyxin may also disrupt the equilibrium between polarity proteins. For example, overexpression of ectopic podocalyxin in OVCAR-3 monolayers caused a bulging of the apical membrane, which may upset the finely tuned balance between apical and basolateral membrane domains, partcularly if it acts co-operatively in association with other depolarizing events. For example, with loss of polarity

93

expansion of podocalyxin down the lateral cell surface may marginalize the basal membrane thereby limiting the surface area capable of forming integrin-mediated contacts which, in effect would cause an 'anti-adhesive' switch. Experimentally, this switch was initiated by maintaining single cells in suspension. However, once could envisage situations in which such a switch could occur when cell-cell interactions were intact, an idea that was supported by experiments carried out in 3-D culture.

In most solid tumours, the dissolution of cell-cell junctions is thought to be an important driver of metastatic dissmemination (Thiery, 2002). However, most ovarian carcinomas express E-cadherin and they often exist as cohesive multicellular aggregates (Naora and Montell, 2005). As a result, I generated multicellular OVCAR-3 and OVCAR-8 aggregates, which exhibit different abilities to polarize appropriately, in 3-D Matrigel culture and assessed the effects of ectopic podocalyxin expression. In polarized aggregates, where podocalyxin localization was apically restricted, $\beta 1$ integrins were appropriately localized at the cell-basement membrane interface. In contrast, in aggregates where polarization did not occur podocalyxin re-localized to the cell-ECM interface and appeared to deplete $\beta 1$ integrin. Therefore, particularly under conditions in which polarity is disrupted, podocalyxin overexpression may perturb integrin engagement at the tumour-stroma interface which would promote metastatic tumour cell shedding into the peritoneal cavity.

In the kidney, podocytes forms focal contacts with the ECM, primarily through $\alpha 3 \beta 1$ integrin (Adler, 1992). High glucose concentrations, which are a characteristic of diabetic nephropathy, lead to a decrease in podocalyxin expression and increased podocyte cell

spreading on a basement membrane substratum *in vitro* as well as foot process effacement *in vivo* (Kanwar et al., 1996; Kanwar et al., 1997; Pagtalunan et al., 1997). In contrast, function blocking β1 integrin antibody treatment disupts cell-ECM interactions and this effect can be ameliorated by simultaneous treatment with the 3D3 podocalyxin antibody (Economou et al., 2004). This led these authors to conclude that podocalyxin competes with β1 integrin-mediated adhesion, which in turn contributes to foot process and slit diaphragm formation by encouraging an expansion of the unattached apical membrane domain of the cells. This expansion phenotype is somewhat reminiscent of the apical bulging that resulted when podocalyxin was overexpressed in OVCAR-3 monolayers and breast carcinoma cell monolayers (Somasiri et al., 2004). Taken together, these data support a mechanism in which podocalyxin exerts its anti-adhesive effects by interfering with integrin-mediated adhesion.

Anti-adhesive effects have also been attributed to mucins, including episialin (MUC1). MUC1 is a molecule that has long been implicated as a tumour cell marker, particularly in breast cancer (Hilkens et al., 1995). Like podocalyxin's proposed mechanism of action, mucins have been shown to exert their anti-adhesive effects by masking the engagement of cell surface adhesion molecules. Although such masking is likely to be more extreme given that MUC1 protrudes approximately 200 to 500 nm above the surface of the cell, depending on the number of mucin repeats (Gendler, 2001). Since this interference occurs as a result of steric hindrance, cell adhesion molecules such as integrins are likely effected in a non-specific manner (Wesseling et al., 1995). As podocalyxin also mediates its anti-adhesive effects via the bulky, negatively charged extracellular domain, it is probable that the anti-adhesive effects are also not specific in terms of the molecules targetted. Thus, it

is possible that all integrin heterodimers are affected, not just the β1 integrins examined in this report.

Anti-adhesive molecules such as MUC1 have been proposed to promote invasion and metastasis (Hilkens et al., 1995). However, for podocalyxin and ovarian cancer, anti-adhesion in the context of tumour dissemination must be reconciled with the adhesive properties adopted by ovarian carcinoma cells that attach to the peritoneal mesothelium. Whether podocalyxin contributes to the later stages of ovarian carcinoma progression is, as yet, unknown. Characterization of podocalyxin expression was carried out on an ovarian TMA, which was composed of primary tumours (B. Gilks, personal communications). Consequently, this analysis did not determine whether podocalyxin is maintained once tumour cells are no longer confined to the ovary. The data I generated from tumourigenic ovarian cell lines suggests that podocalyxin expression can be extremely variable. Therefore, during the later stages of ovarian carcinoma metastasis podocalyxin expression could be downregulated or podocalyxin could be cleaved and/or shed from the membrane, as was evident in several primary tumours present on the TMA. Alternatively, once ovarian carcinoma cells have seeded the peritoneal cavity, podocalyxin's anti-adhesive effects could be influenced by factors present in the ascitic microenvironment.

Ascites is a common characteristic of ovarian cancer caused by the accumulation of fluid in the peritoneal cavity due to imbalances between influx and efflux from the peritoneal compartment. Ascites contains a variety of growth factors, extracellular matrix components, chemokines and cytokines that are secreted by tumour cells, tumour-infiltrating leukocytes,

and activated mesothelial cells (Offner et al., 1995). The complex assortment of factors in ascites can induce functional changes in the behaviour of ovarian carcinoma cells. For example, ascites has been demonstrated to induce increased expression of the $\alpha6$ integrin subunit (Ahmed et al., 2005). Thus, once exposed to ascites in the peritoneal cavity, ascites-induced increases in integrin expression may upregulate the presence of adhesive receptors, which could overcome the anti-adhesive effects of podocalyxin. Such a change in the adhesive balance would, potentially, increase the probability of secondary attachment to the peritoneal wall.

Other ascites-induced changes to the behaviour of ovarian carcinoma cells have the potential to overcome the effects of anti-adhesins like podocalyxin. Lysophosphatidic acid (LPA) is a phospholipid ligand that activates G-protein coupled receptors to induce many cellular responses. High levels of LPA have been observed in the ascites of ovarian cancer patients (Mills et al., 1988; Xu et al., 1995). *In vitro*, LPA stimulates a number of cellular effects that promote the tumourigenicity of ovarian carcinoma cells including induction of cell motility and invasion (Fishman et al., 2001; Sawada et al., 2002). Interestingly, LPA treatment of ovarian cancer cell lines has been reported to stimulate expression of cytokines interleukin-6 (IL-6) and interleukin-8 (IL-8) (Fang et al., 2004). IL-6 and IL-8 occur at higher concentrations in the ascites of ovarian carcinoma patients than in the serum, suggesting that ovarian carcinoma cells in the ascites are the source of this cytokine production (Penson et al., 2000). Cytokine signalling could regulate the localization of anti-adhesins such as podocalyxin and its scaffolding proteins through activation-dependent changes to the actin cytoskeleton. For example, interleukin-3 (IL-3) treatment of

hematopoietic stem cells in suspension culture enhances the clustering of podocalyxin and NHERF-1 into a polarized membrane microdomain 'cap' (Tan et al., 2006). Thus, it will be interesting to determine if cytokine-induced segregation of podocalyxin can unmask adhesive molecules in suspended ovarian carcinoma cells such that integrin-dependent adhesion to peritoneal cells is restored.

The data presented here indicates that podocalyxin is expressed by the overwhelming majority of epithelial ovarian carcinomas confined to the ovary. However, this expression did not serve as a prognostic indicator of outcome. Despite the latter observation, podocalyxin overexpression in OVCAR-3 ovarian carcinoma cells caused defects in cell-cell aggregation and it dramatically reduced cell adhesion to the extracellular matrix and peritoneal cell monolayers. On its own podocalyxin did not disrupt polarity or greatly influence adherens junctions dynamics in cell monolayers. In non-polar 3D clusters, podocalyxin localized to the cell-ECM interface, resulting in a depletion of $\beta 1$ integrin from this domain. Taken together, these data suggest that in cellular contexts where podocalyxin localizes asymmetrically it restricts the distribution of integrins, whereas in situations where podocalyxin is distributed evenly to the cell surface, it interferes with integrin engagement. Since podocalyxin expression is prevalent among primary ovarian carcinoma, its anti-adhesive, integrin-masking effects may facilitate tumor cell shedding, thereby promoting the first stages of metastasis.

REFERENCES

Abdullah, K.M,. Udoh, E.A., Shewen, P.E., and Mellors, A. (1992). A neutral glycoprotease of Pasteurella haemolytica A1 specifically cleaves O-sialoglycoproteins. Infect Immun *60*, 56-62.

Adams, C. L., Chen, Y. T., Smith, S. J., and Nelson, W. J. (1998). Mechanisms of epithelial cell-cell adhesion and cell compaction revealed by high-resolution tracking of E-cadherin-green fluorescent protein. J Cell Biol *142*, 1105-1119.

Adams, C. L., Nelson, W. J., and Smith, S. J. (1996). Quantitative analysis of cadherin-catenin-actin reorganization during development of cell-cell adhesion. J Cell Biol *135*, 1899-1911.

Adler, S. (1992). Characterization of glomerular epithelial cell matrix receptors. Am J Pathol *141*, 571-578.

Ahmed, N., Riley, C., Oliva, K., Rice, G., and Quinn, M. (2005). Ascites induces modulation of alpha6beta1 integrin and urokinase plasminogen activator receptor expression and associated functions in ovarian carcinoma. Br J Cancer *92*, 1475-1485.

Allen, H.J., Porter, C., Gamarra, M., Piver, M.S., Johnson, E.A. (1987). Isolation and morphologic characterization of human ovarian carcinoma cell clusters present in effusions. Exp Cell Biol *55*, 194-208.

Ando-Akatsuka, Y., Yonemura, S., Itoh, M., Furuse, M., and Tsukita, S. (1999). Differential behavior of E-cadherin and occludin in their colocalization with ZO-1 during the establishment of epithelial cell polarity. J Cell Physiol *179*, 115-125.

Auersperg, N., Pan, J., Grove, B. D., Peterson, T., Fisher, J., Maines-Bandiera, S., Somasiri, A., and Roskelley, C. D. (1999). E-cadherin induces mesenchymal-to-epithelial transition in human ovarian surface epithelium. Proc Natl Acad Sci U S A *96*, 6249-6254.

Auersperg, N., Wong, A. S., Choi, K. C., Kang, S. K., and Leung, P. C. (2001). Ovarian surface epithelium: biology, endocrinology, and pathology. Endocr Rev *22*, 255-288.

Baas, A. F., Kuipers, J., van der Wel, N. N., Batlle, E., Koerten, H. K., Peters, P. J., and Clevers, H. C. (2004). Complete polarization of single intestinal epithelial cells upon activation of LKB1 by STRAD. Cell *116*, 457-466.

Barber, H. R. (1993). Prophylaxis in ovarian cancer. Cancer *71*, 1529-1533.

Becker, J. W., Erickson, H. P., Hoffman, S., Cunningham, B. A., and Edelman, G. M. (1989). Topology of cell adhesion molecules. Proc Natl Acad Sci U S A *86*, 1088-1092.

Berryman, M., Franck, Z., and Bretscher, A. (1993). Ezrin is concentrated in the apical microvilli of a wide variety of epithelial cells whereas moesin is found primarily in endothelial cells. J Cell Sci *105 (Pt 4)*, 1025-1043.

Birchmeier, W., and Behrens, J. (1994). Cadherin expression in carcinomas: role in the formation of cell junctions and the prevention of invasiveness. Biochim Biophys Acta *1198*, 11-26.

Burleson, K. M., Casey, R. C., Skubitz, K. M., Pambuccian, S. E., Oegema, T. R., Jr., and Skubitz, A. P. (2004). Ovarian carcinoma ascites spheroids adhere to extracellular matrix components and mesothelial cell monolayers. Gynecol Oncol *93*, 170-181.

Cannistra, S. A., Ottensmeier, C., Niloff, J., Orta, B., and DiCarlo, J. (1995). Expression and function of beta 1 and alpha v beta 3 integrins in ovarian cancer. Gynecol Oncol *58*, 216-225.

Darai, E., Scoazec, J. Y., Walker-Combrouze, F., Mlika-Cabanne, N., Feldmann, G., Madelenat, P., and Potet, F. (1997). Expression of cadherins in benign, borderline, and malignant ovarian epithelial tumors: a clinicopathologic study of 60 cases. Hum Pathol *28*, 922-928.

Davidson, B., Berner, A., Nesland, J. M., Risberg, B., Berner, H. S., Trope, C. G., Kristensen, G. B., Bryne, M., and Ann Florenes, V. (2000). E-cadherin and alpha-, beta-and gamma-catenin protein expression is up-regulated in ovarian carcinoma cells in serous effusions. J Pathol *192*, 460-469.

Davies, B. R., Worsley, S. D., and Ponder, B. A. (1998). Expression of E-cadherin, alpha-catenin and beta-catenin in normal ovarian surface epithelium and epithelial ovarian cancers. Histopathology *32*, 69-80.

Dekan, G., Gabel, C., and Farquhar, M. G. (1991). Sulfate contributes to the negative charge of podocalyxin, the major sialoglycoprotein of the glomerular filtration slits. Proc Natl Acad Sci U S A *88*, 5398-5402.

Doyonnas, R., Kershaw, D. B., Duhme, C., Merkens, H., Chelliah, S., Graf, T., and McNagny, K. M. (2001). Anuria, omphalocele, and perinatal lethality in mice lacking the CD34-related protein podocalyxin. J Exp Med *194*, 13-27.

Ebnet, K., Suzuki, A., Horikoshi, Y., Hirose, T., Meyer Zu Brickwedde, M. K., Ohno, S., and Vestweber, D. (2001). The cell polarity protein ASIP/PAR-3 directly associates with junctional adhesion molecule (JAM). Embo J *20*, 3738-3748.

Ebnet, K., Suzuki, A., Ohno, S., and Vestweber, D. (2004). Junctional adhesion molecules (JAMs): more molecules with dual functions? J Cell Sci *117*, 19-29.

Economou, C. G., Kitsiou, P. V., Tzinia, A. K., Panagopoulou, E., Marinos, E., Kershaw, D. B., Kerjaschki, D., and Tsilibary, E. C. (2004). Enhanced podocalyxin expression alters the structure of podocyte basal surface. J Cell Sci *117*, 3281-3294.

Eder, A. M., Sui, X., Rosen, D. G., Nolden, L. K., Cheng, K. W., Lahad, J. P., Kango-Singh, M., Lu, K. H., Warneke, C. L., Atkinson, E. N., *et al.* (2005). Atypical PKCiota contributes to poor prognosis through loss of apical-basal polarity and cyclin E overexpression in ovarian cancer. Proc Natl Acad Sci U S A *102*, 12519-12524.

Fang, X., Yu, S., Bast, R.C., Liu, S., Xu, H.J., Hu, S.X., LaPushin, R., Claret, F.X., Aggarwal, B.B., Lu, Y., and Mills, G.B. (2000). Lysophospholipid growth factors in the initiation, progression, metastases, and management of ovarian cancer. Ann N Y Acad Sci *905*, 188-208.

Feeley, K. M., and Wells, M. (2001). Precursor lesions of ovarian epithelial malignancy. Histopathology *38*, 87-95.

Fishman, D. A., Liu, Y., Ellerbroek, S. M., and Stack, M. S. (2001). Lysophosphatidic acid promotes matrix metalloproteinase (MMP) activation and MMP-dependent invasion in ovarian cancer cells. Cancer Res *61*, 3194-3199.

Fukata, M., and Kaibuchi, K. (2001). Rho-family GTPases in cadherin-mediated cell-cell adhesion. Nat Rev Mol Cell Biol *2*, 887-897.

Fukuhara, A., Irie, K., Yamada, A., Katata, T., Honda, T., Shimizu, K., Nakanishi, H., and Takai, Y. (2002). Role of nectin in organization of tight junctions in epithelial cells. Genes Cells *7*, 1059-1072.

Gendler, S.J. (2001). MUC1, the renaissance molecule. J Mammary Gland Biol Neoplasia *6*, 339-53.

Gumbiner, B. (1988). Cadherins: a family of Ca2+-dependent adhesion molecules. Trends Biochem Sci *13*, 75-76.

Hemminki, A., Markie, D., Tomlinson, I., Avizienyte, E., Roth, S., Loukola, A., Bignell, G., Warren, W., Aminoff, M., Hoglund, P., *et al.* (1998). A serine/threonine kinase gene defective in Peutz-Jeghers syndrome. Nature *391*, 184-187.

Hilkens, J., Vos, H. L., Wesseling, J., Boer, M., Storm, J., van der Valk, S., Calafat, J., and Patriarca, C. (1995). Is episialin/MUC1 involved in breast cancer progression? Cancer Lett *90*, 27-33.

Hinck, L., Nathke, I.S., Papkoff, J., and Nelson, W.J. (1994). Dynamics of cadherin/catenin complex formation: novel protein interactions and pathways of complex assembly. J Cell Biol *125*, 1327-40.

Horvat, R., Hovorka, A., Dekan, G., Poczewski, H., and Kerjaschki, D. (1986). Endothelial cell membranes contain podocalyxin--the major sialoprotein of visceral glomerular epithelial cells. J Cell Biol *102*, 484-91.

Hough, C. D., Sherman-Baust, C. A., Pizer, E. S., Montz, F. J., Im, D. D., Rosenshein, N. B., Cho, K. R., Riggins, G. J., and Morin, P. J. (2000). Large-scale serial analysis of gene expression reveals genes differentially expressed in ovarian cancer. Cancer Res *60*, 6281-6287.

Hynes, R. O. (1992). Integrins: versatility, modulation, and signaling in cell adhesion. Cell *69*, 11-25.

Inoue, M., Ogawa, H., Miyata, M., Shiozaki, H., and Tanizawa, O. (1992). Expression of E-cadherin in normal, benign, and malignant tissues of female genital organs. Am J Clin Pathol *98*, 76-80.

Izumi, Y., Hirose, T., Tamai, Y., Hirai, S., Nagashima, Y., Fujimoto, T., Tabuse, Y., Kemphues, K. J., and Ohno, S. (1998). An atypical PKC directly associates and colocalizes at the epithelial tight junction with ASIP, a mammalian homologue of Caenorhabditis elegans polarity protein PAR-3. J Cell Biol *143*, 95-106.

Jenne, D. E., Reimann, H., Nezu, J., Friedel, W., Loff, S., Jeschke, R., Muller, O., Back, W., and Zimmer, M. (1998). Peutz-Jeghers syndrome is caused by mutations in a novel serine threonine kinase. Nat Genet *18*, 38-43.

Joberty, G., Petersen, C., Gao, L., and Macara, I. G. (2000). The cell-polarity protein Par6 links Par3 and atypical protein kinase C to Cdc42. Nat Cell Biol *2*, 531-539.

Kanwar, Y. S., Liu, Z. Z., Kumar, A., Usman, M. I., Wada, J., and Wallner, E. I. (1996). D-glucose-induced dysmorphogenesis of embryonic kidney. J Clin Invest *98*, 2478-2488.

Kanwar, Y. S., Liu, Z. Z., and Wallner, E. I. (1997). Influence of glucose on murine metanephric development and proteoglycans: morphologic and biochemical studies. Lab Invest *76*, 671-681.

Kerjaschki, D., Sharkey, D. J., and Farquhar, M. G. (1984). Identification and characterization of podocalyxin--the major sialoprotein of the renal glomerular epithelial cell. J Cell Biol *98*, 1591-1596.

Kershaw, D. B., Beck, S. G., Wharram, B. L., Wiggins, J. E., Goyal, M., Thomas, P. E., and Wiggins, R. C. (1997). Molecular cloning and characterization of human podocalyxin-like protein. Orthologous relationship to rabbit PCLP1 and rat podocalyxin. J Biol Chem *272*, 15708-15714.

Kleinman, H. K., McGarvey, M. L., Liotta, L. A., Robey, P. G., Tryggvason, K., and Martin, G. R. (1982). Isolation and characterization of type IV procollagen, laminin, and heparan sulfate proteoglycan from the EHS sarcoma. Biochemistry *21*, 6188-6193.

Knust, E., and Bossinger, O. (2002). Composition and formation of intercellular junctions in epithelial cells. Science *298*, 1955-1959.

Lessan, K., Aguiar, D. J., Oegema, T., Siebenson, L., and Skubitz, A. P. (1999). CD44 and beta1 integrin mediate ovarian carcinoma cell adhesion to peritoneal mesothelial cells. Am J Pathol *154*, 1525-1537.

Li, Y., Li, J., Straight, S.W., and Kershaw, D.B. (2001) PDZ domain-mediated interaction of rabbit podocalyxin and Na(+)/H(+) exchange regulatory factor-2. Am J Physiol Renal Physiol *282*, 1129-39.

Lin, D., Edwards, A. S., Fawcett, J. P., Mbamalu, G., Scott, J. D., and Pawson, T. (2000). A mammalian PAR-3-PAR-6 complex implicated in Cdc42/Rac1 and aPKC signalling and cell polarity. Nat Cell Biol *2*, 540-547.

Maines-Bandiera, S. L., and Auersperg, N. (1997). Increased E-cadherin expression in ovarian surface epithelium: an early step in metaplasia and dysplasia? Int J Gynecol Pathol *16*, 250-255.

Martin, S. G., and St Johnston, D. (2003). A role for Drosophila LKB1 in anterior-posterior axis formation and epithelial polarity. Nature *421*, 379-384.

Matter, K., and Balda, M. S. (2003). Functional analysis of tight junctions. Methods *30*, 228-234.

McNagny, K. M., Pettersson, I., Rossi, F., Flamme, I., Shevchenko, A., Mann, M., and Graf, T. (1997). Thrombomucin, a novel cell surface protein that defines thrombocytes and multipotent hematopoietic progenitors. J Cell Biol *138*, 1395-1407.

Meder, D., Shevchenko, A., Simons, K., and Fullekrug, J. (2005). Gp135/podocalyxin and NHERF-2 participate in the formation of a preapical domain during polarization of MDCK cells. J Cell Biol *168*, 303-313.

Mills, G. B., May, C., McGill, M., Roifman, C. M., and Mellors, A. (1988). A putative new growth factor in ascitic fluid from ovarian cancer patients: identification, characterization, and mechanism of action. Cancer Res *48*, 1066-1071.

Mittal, K. R., Zeleniuch-Jacquotte, A., Cooper, J. L., and Demopoulos, R. I. (1993). Contralateral ovary in unilateral ovarian carcinoma: a search for preneoplastic lesions. Int J Gynecol Pathol *12*, 59-63.

Naora, H., and Montell, D. J. (2005). Ovarian cancer metastasis: integrating insights from disparate model organisms. Nat Rev Cancer *5*, 355-366.

Nelson, W. J. (2003). Adaptation of core mechanisms to generate cell polarity. Nature *422*, 766-774.

Nielsen, J.S., McCoy, M.L., Chelliah, S., Vogl, A.W., Roskelley, C.D., and McNagny, K.M. (2005). Ectopic expression of a single protein is sufficient to drive microvillus formation. *45th Annual Meeting for the American Society for Cell Biology.* San Francisco, CA.

O'Brien, L. E., Jou, T. S., Pollack, A. L., Zhang, Q., Hansen, S. H., Yurchenco, P., and Mostov, K. E. (2001). Rac1 orientates epithelial apical polarity through effects on basolateral laminin assembly. Nat Cell Biol *3*, 831-838.

Offner, F. A., Obrist, P., Stadlmann, S., Feichtinger, H., Klingler, P., Herold, M., Zwierzina, H., Hittmair, A., Mikuz, G., Abendstein, B., and et al. (1995). IL-6 secretion by human peritoneal mesothelial and ovarian cancer cells. Cytokine *7*, 542-547.

Ojakian, G. K., and Schwimmer, R. (1988). The polarized distribution of an apical cell surface glycoprotein is maintained by interactions with the cytoskeleton of Madin-Darby canine kidney cells. J Cell Biol *107*, 2377-2387.

Ojakian, G. K., and Schwimmer, R. (1994). Regulation of epithelial cell surface polarity reversal by beta 1 integrins. J Cell Sci *107 (Pt 3)*, 561-576.

Orsulic, S., Li, Y., Soslow, R. A., Vitale-Cross, L. A., Gutkind, J. S., and Varmus, H. E. (2002). Induction of ovarian cancer by defined multiple genetic changes in a mouse model system. Cancer Cell *1*, 53-62.

Pagtalunan, M. E., Miller, P. L., Jumping-Eagle, S., Nelson, R. G., Myers, B. D., Rennke, H. G., Coplon, N. S., Sun, L., and Meyer, T. W. (1997). Podocyte loss and progressive glomerular injury in type II diabetes. J Clin Invest *99*, 342-348.

Penson, R. T., Kronish, K., Duan, Z., Feller, A. J., Stark, P., Cook, S. E., Duska, L. R., Fuller, A. F., Goodman, A. K., Nikrui, N., *et al.* (2000). Cytokines IL-1beta, IL-2, IL-6, IL-8, MCP-1, GM-CSF and TNFalpha in patients with epithelial ovarian cancer and their relationship to treatment with paclitaxel. Int J Gynecol Cancer *10*, 33-41.

Pinal, N., Goberdhan, D. C., Collinson, L., Fujita, Y., Cox, I. M., Wilson, C., and Pichaud, F. (2006). Regulated and polarized PtdIns(3,4,5)P3 accumulation is essential for apical membrane morphogenesis in photoreceptor epithelial cells. Curr Biol *16*, 140-149.

Pinkas, J., and Leder, P. (2002). MEK1 signaling mediates transformation and metastasis of EpH4 mammary epithelial cells independent of an epithelial to mesenchymal transition. Cancer Res *62*, 4781-4790.

Reddy, P., Liu, L., Ren, C., Lindgren, P., Boman, K., Shen, Y., Lundin, E., Ottander, U., Rytinki, M., and Liu, K. (2005). Formation of E-cadherin-mediated cell-cell adhesion activates AKT and mitogen activated protein kinase via phosphatidylinositol 3 kinase and ligand-independent activation of epidermal growth factor receptor in ovarian cancer cells. Mol Endocrinol *19*, 2564-2578.

Roskelley, C. D., and Bissell, M. J. (2002). The dominance of the microenvironment in breast and ovarian cancer. Semin Cancer Biol *12*, 97-104.

Salazar, H., Godwin, A. K., Daly, M. B., Laub, P. B., Hogan, W. M., Rosenblum, N., Boente, M. P., Lynch, H. T., and Hamilton, T. C. (1996). Microscopic benign and invasive malignant neoplasms and a cancer-prone phenotype in prophylactic oophorectomies. J Natl Cancer Inst *88*, 1810-1820.

Sassetti, C., Tangemann, K., Singer, M. S., Kershaw, D. B., and Rosen, S. D. (1998). Identification of podocalyxin-like protein as a high endothelial venule ligand for L-selectin: parallels to CD34. J Exp Med *187*, 1965-1975.

Sawada, H., Stukenbrok, H., Kerjaschki, D., and Farquhar, M. G. (1986). Epithelial polyanion (podocalyxin) is found on the sides but not the soles of the foot processes of the glomerular epithelium. Am J Pathol *125*, 309-318.

Sawada, K., Morishige, K., Tahara, M., Ikebuchi, Y., Kawagishi, R., Tasaka, K., and Murata, Y. (2002). Lysophosphatidic acid induces focal adhesion assembly through Rho/Rho-associated kinase pathway in human ovarian cancer cells. Gynecol Oncol *87*, 252-259.

Schnabel, E., Dekan, G., Miettinen, A., and Farquhar, M. G. (1989). Biogenesis of podocalyxin--the major glomerular sialoglycoprotein--in the newborn rat kidney. Eur J Cell Biol *48*, 313-326.

Schwimmer, R., and Ojakian, G. K. (1995). The alpha 2 beta 1 integrin regulates collagen-mediated MDCK epithelial membrane remodeling and tubule formation. J Cell Sci *108 (Pt 6)*, 2487-2498.

Scully, R. E. (1995). Early de novo ovarian cancer and cancer developing in benign ovarian lesions. Int J Gynaecol Obstet *49 Suppl*, S9-15.

Seltzer, J. L., Lee, A. Y., Akers, K. T., Sudbeck, B., Southon, E. A., Wayner, E. A., and Eisen, A. Z. (1994). Activation of 72-kDa type IV collagenase/gelatinase by normal fibroblasts in collagen lattices is mediated by integrin receptors but is not related to lattice contraction. Exp Cell Res *213*, 365-374.

Shibata, T., Chuma, M., Kokubu, A., Sakamoto, M., and Hirohashi, S. (2003). EBP50, a beta-catenin-associating protein, enhances Wnt signaling and is over-expressed in hepatocellular carcinoma. Hepatology *38*, 178-186.

Somasiri, A., Nielsen, J. S., Makretsov, N., McCoy, M. L., Prentice, L., Gilks, C. B., Chia, S. K., Gelmon, K. A., Kershaw, D. B., Huntsman, D. G., *et al.* (2004). Overexpression of the anti-adhesin podocalyxin is an independent predictor of breast cancer progression. Cancer Res *64*, 5068-5073.

Sundfeldt, K., Ivarsson, K., Rask, K., Haeger, M., Hedin, L., and Brannstrom, M. (2001). Higher levels of soluble E-cadherin in cyst fluid from malignant ovarian tumours than in benign cysts. Anticancer Res *21*, 65-70.

Sundfeldt, K., Piontkewitz, Y., Ivarsson, K., Nilsson, O., Hellberg, P., Brannstrom, M., Janson, P. O., Enerback, S., and Hedin, L. (1997). E-cadherin expression in human epithelial ovarian cancer and normal ovary. Int J Cancer *74*, 275-280.

Sutherland, D.R., Abdullah, K.M., Cyopick, P., and Mellors, A. (1992). Cleavage of the cell-surface O-sialoglycoproteins CD34, CD43, CD44, and CD45 by a novel glycoprotease from Pasteurella haemolytica. J Immunol 148, 1458-64.

Suzuki, A., Yamanaka, T., Hirose, T., Manabe, N., Mizuno, K., Shimizu, M., Akimoto, K., Izumi, Y., Ohnishi, T., and Ohno, S. (2001). Atypical protein kinase C is involved in the evolutionarily conserved par protein complex and plays a critical role in establishing epithelia-specific junctional structures. J Cell Biol *152*, 1183-1196.

Takada, Y., and Puzon, W. (1993). Identification of a regulatory region of integrin beta 1 subunit using activating and inhibiting antibodies. J Biol Chem *268*, 17597-17601.

Takahashi, Y., Morales, F. C., Kreimann, E. L., and Georgescu, M. M. (2006). PTEN tumor suppressor associates with NHERF proteins to attenuate PDGF receptor signaling. Embo J *25*, 910-920.

Takeda, T., Go, W. Y., Orlando, R. A., and Farquhar, M. G. (2000). Expression of podocalyxin inhibits cell-cell adhesion and modifies junctional properties in Madin-Darby canine kidney cells. Mol Biol Cell *11*, 3219-3232.

Takeda, T., McQuistan, T., Orlando, R. A., and Farquhar, M. G. (2001). Loss of glomerular foot processes is associated with uncoupling of podocalyxin from the actin cytoskeleton. J Clin Invest *108*, 289-301.

Tan, P. C., Furness, S. G., Merkens, H., Lin, S., McCoy, M. L., Roskelley, C. D., Kast, J., and McNagny, K. M. (2006). Na+/H+ exchanger regulatory factor-1 is a hematopoietic ligand for a subset of the CD34 family of stem cell surface proteins. Stem Cells *24*, 1150-1161.

Tortolero-Luna, G., and Mitchell, M. F. (1995). The epidemiology of ovarian cancer. J Cell Biochem Suppl *23*, 200-207.

Tresserra, F., Grases, P. J., Labastida, R., and Ubeda, A. (1998). Histological features of the contralateral ovary in patients with unilateral ovarian cancer: a case control study. Gynecol Oncol *71*, 437-441.

Thiery, J.P. (2002). Epithelial-mesenchymal transitions in tumour progression. Nat Rev Cancer *2*, 442-54.

Wang, A. Z., Ojakian, G. K., and Nelson, W. J. (1990). Steps in the morphogenesis of a polarized epithelium. II. Disassembly and assembly of plasma membrane domains during reversal of epithelial cell polarity in multicellular epithelial (MDCK) cysts. J Cell Sci *95 (Pt 1)*, 153-165.

Watts, J. L., Morton, D. G., Bestman, J., and Kemphues, K. J. (2000). The C. elegans par-4 gene encodes a putative serine-threonine kinase required for establishing embryonic asymmetry. Development *127*, 1467-1475.

Weaver, V. M., Petersen, O. W., Wang, F., Larabell, C. A., Briand, P., Damsky, C., and Bissell, M. J. (1997). Reversion of the malignant phenotype of human breast cells in three-dimensional culture and in vivo by integrin blocking antibodies. J Cell Biol *137*, 231-245.

Weinman, E. J. (2001). New functions for the NHERF family of proteins. J Clin Invest *108*, 185-186.

Wesseling, J., van der Valk, S. W., and Hilkens, J. (1996). A mechanism for inhibition of E-cadherin-mediated cell-cell adhesion by the membrane-associated mucin episialin/MUC1. Mol Biol Cell *7*, 565-577.

Wesseling, J., van der Valk, S. W., Vos, H. L., Sonnenberg, A., and Hilkens, J. (1995). Episialin (MUC1) overexpression inhibits integrin-mediated cell adhesion to extracellular matrix components. J Cell Biol *129*, 255-265.

Xu, Y., Gaudette, D. C., Boynton, J. D., Frankel, A., Fang, X. J., Sharma, A., Hurteau, J., Casey, G., Goodbody, A., Mellors, A., and et al. (1995). Characterization of an ovarian cancer activating factor in ascites from ovarian cancer patients. Clin Cancer Res *1*, 1223-1232.

Yeaman, C., Grindstaff, K. K., and Nelson, W. J. (1999). New perspectives on mechanisms involved in generating epithelial cell polarity. Physiol Rev *79*, 73-98.

Yokoyama, S., Tachibana, K., Nakanishi, H., Yamamoto, Y., Irie, K., Mandai, K., Nagafuchi, A., Monden, M., and Takai, Y. (2001). alpha-catenin-independent recruitment of ZO-1 to nectin-based cell-cell adhesion sites through afadin. Mol Biol Cell *12*, 1595-1609.

Yonemura, S., Itoh, M., Nagafuchi, A., and Tsukita, S. (1995). Cell-to-cell adherens junction formation and actin filament organization: similarities and differences between non-polarized fibroblasts and polarized epithelial cells. J Cell Sci *108 (Pt 1)*, 127-142.

Zegers, M. M., O'Brien, L. E., Yu, W., Datta, A., and Mostov, K. E. (2003). Epithelial polarity and tubulogenesis in vitro. Trends Cell Biol *13*, 169-176.